Diffusion-Mediated Regulation of Endocrine Networks

A Thesis by

Danny Petrasek

In Partial Fulfillment of the Requirements

for the Degree of

Doctor of Philosophy

California Institute of Technology

Pasadena, California

March 4 2002

(Defended)

"The rate of diffusion and the diffusion-path-length of various metabolites and enzymes are believed to set physical limits on the size and volume of the metabolizing mass of living cells and their organelles."

Lehninger's Biochemistry 1975, p.79

Acknowledgements

It is particularly difficult for me to compress onto a few pages my gratitude to all the important people that contributed to my safe arrival across the "trans-disciplinary" sea. First I wish to thank my advisor Professor Donald Cohen. I was exceptionally privileged to have had Don Cohen as a mentor and friend. Don embodied the Caltech experience for me. He was a grandmaster in the art of nurturing interesting ideas and then tempering them to withstand the heat of scientific rigor. The experience I gained from training with a world class mathematical modeler and scientist was and remains a priceless treasure. I hope to continue learning from you. Thank you Don.

I was equally fortunate to be blessed with a second mentor, Professor Scott Fraser, who served as a co-advisor and a constant source of inspiration throughout my entire Caltech graduate school experience. Scott Fraser is an extraordinary intellect, scientist and teacher. It will be impossible to list the countless insights I gained from our discussions. I am further indebted to Scott for his never wavering confidence in my quest to bridge the biological/mathematical gulf. His kindness and generosity was and remains boundless and always carefully disguised in his legendary wit. Nothing would please me more than to continue our friendship and scientific collaboration. I wish to thank Dr. Ravi Samtaney, my collaborator, dear friend and teacher. Ravi was a most powerful catalyst in making the research enjoyable and exciting. I hope we continue on for the next many years.

There are many many friends and scientists that I would like to mention and will not be able to do justice to their contribution. I want to thank Alan Garfinkel, Linda Demer, Bill Goodman, Isidro Salusky, Andre Van Herle, Oscar Bruno, Mel Simon, Henry Lester, Paul Sternberg, Michael Carey, Dimitri Vaymblatt, Maya Tokman, Chad Schmutzer, Sheila Shull, Georgia Frueh, Roni Goldring, Sam Bornstein, Amos Feldman, David Affeld, Eugene Chudin, Debbi Petrasek, Jon Chapman, Irwin Kurland, Elena Zhukova, Girard Jensen, Naftali Stern, Patrick Guidotti, John Pelesko, leonid Kunyansky, Gang Hu, Tom Hou, Dan Meiron, Randy Paffenroth, Julian Chaubel,Razvan Fetecau, Andy Greenberg, My family (Vered, Petrasek, Swerdlow, Seliktar, Geiger, Friedmann) and to all the unmentioned please forgive me.

Finally, I wish to thank some very special people that were instrumental in helping me. I want to thank my dearest friend Lenny Rudin, whose constant source of encouragement and inspiration eased my survival during these years. I want to thank my Parents, Martin and Adrianna, whose love fueled my ambition. I would like to thank my most precious daughter, Alexandra Rachel, for bringing the meaning of my life to its highest octave.

This thesis is dedicated to the loving memory of my Grandparents Eugene and Lilly Schoenberger who I was blessed to know and love, to my son Adiel who I was blessed to know briefly and to my Grandparents Chaim and Esther Friedman who I have only known in my prayers and thoughts.

Abstract

In endocrine glands, vigorous and coordinated responses are often elicited by modest changes in the concentration of the organist molecule. The mammalian parathyroid gland is a representative case. Small (5%) changes in serum calcium result in tenfold (1000%) changes in glandular parathyroid hormone (PTH) release. In vitro, single isolated cells are observed to secrete fewer hormones than cells residing within a connected group, suggesting that a network has emergent regulatory properties. In PTH secreting tumors however, the ability to quickly respond to changes in calcium is strongly damped. A unifying hypothesis that accounts for these phenomena is realized by extra-cellular modulation of calcium diffusivity. A theoretical model and computational experiments demonstrate qualitative agreement with published experimental results. Our results suggest that in addition to the cellular mechanisms, endocrine glandular networks may have regulatory prowess at the level of interstitial transport. The extra-cellular diffusional mechanism proposed provides a consistent argument for 1) higher secretion of single cells in a connected network compared to isolated cells, 2) the rapid nonlinear response seen in healthy glands as well as 3) the pathological responses seen in hyperplasia and adenoma. Since the proposed diffusional regulation strongly depends on the existence of a connected cell network (gland), it also suggests a rationale for the advantages of cell networks as organs versus a dispersed system of isolated cells (in the case of the parathyroid gland).

Contents

List of Figures

List of Tables

0.1 Preface

In our time it has become almost routine medical practice to replace failing or dysfunctional organs by transplantation. It is interesting to note that in almost every case when there is a choice between human tissue and a synthetic substitute, the "natural" organ is preferred because of superior practical results, underscoring the incompleteness of our fundamental biological knowledge. Living organs in general not only have material and structural properties, but in most cases generate biological products that are exported to the rest of the organism. Processes that involve the intracellular synthesis of biologically active molecules for the purpose of export to other cells define endocrine systems. In mammals, the export and delivery is primarily carried out by a circulatory system. Specialized organs whose function is exclusively to export these molecules or hormones are defined as endocrine glands. If we assume that evolutionary or physical forces have guided the shape and arrangement of mammalian endocrine glands, we are then confronted with a natural question. What is special or advantageous about this design versus some other design? Posing such a question in biology requires it be considered in the proper context. For example, in considering biological advantages of having multiple immune glands (lymph nodes) dispersed around the animal body, an answer that accounts strictly for local biochemical and cell biology phenomena may be insufficient in its explanation at the scale of the system or (whole body) properties. Theoretical models continually attempt to reconcile the various disparate features of a studied scientific problem. The physiological hypothesis and model submitted here is offered with the point of view that regardless of its eventual validation or refutation, it will for the moment serve as a rational explanation for a spectrum of parathyroid gland physiological phenomena. If only by its existence and not its validity it inspires experiments that clarify paradoxical results or bring a new understanding in hormone regulation, the work will have served its purpose.

0.2 Outline of the thesis

This section will serve as an outline of the thesis. It is intended to provide the reader with an overview as to the contents of each section and also as a guide regarding the strategy of the presentation. The emphasis of this work has been to establish a mathematical model for understanding and reconciling a collection of physiological phenomena. The physiology

investigated here is responsible for the healthy maintenance of calcium in humans. The physiological questions to be addressed are divided into two categories: a cell-level (microphysiology) and a whole gland-level (macrophysiology). As such, separate but related mathematical models have been constructed.

1. Chapter one will be divided into two parts.

   - Part one will begin with a succinct introduction and background to the glandular-level physiology and the related scientific questions. The phenomena of interest are then summarized in a list.

   - Part two will introduce the cell-level physiology with a brief discussion of relevant results from the literature. A list of the main cellular physiological phenomena is again provided.

     At the end of the thesis a modest amount of supplementary reference material from the biomedical literature is provided. This was done so that the thesis would be a self contained reference. The model construction required an extensive survey of results from a wide range of biological topics. The assumptions and considerations made in the model construction are drawn from this literature. The reader may choose to refer to this material as needed.

   - In chapter two we will state our physiological hypothesis. The system of cell level model equations are then given. The assumptions that are made are justified throughout. The numerical methods used are then described.

   - In chapter three simulations analogous to the important cell-level physiology are shown. In particular they are as follows:

     - The secretory response of isolated single cells vs the response of an average cell residing in a group.
     - The differences in the secretory response of cells with respect to cell spacing.
     - The secretory response of a PTH secreting tumor: whole tumor vs the fragmented cell collections.

     A summary and discussion of the results follow.

- In chapter four, the glandular-level model is constructed. The system of equations are given and a discussion of the assumptions follows. The numerical methods are then described.
- In chapter five simulations that parallel clinical studies from the medical literature and from our UCLA collaborators are shown. These broadly cover the following:
  - Simulations comparing infusion studies on "healthy" parathyroid glands.
  - Simulations comparing infusion studies on pathological glands.
  - Simulations using UCLA patient data.
  - A brief discussion relating a clinical observation.
- In chapter six, a more refined cellular-level model is presented. Simulations comparable to the first model are shown.
- In chapter seven future research objectives and thoughts are entertained.
- Chapter eight is devoted to concluding remarks.
- Chapter nine is the supplementary material.

Chapter 1 Background and Significance

1.1 Synopsis of the glandular level physiology

1.1.1 General information about calcium and the parathyroid hormone (PTH)

The role of calcium molecules in biological processes is ubiquitous [51]. In mammalian physiology, countless calcium signaling events are taking place simultaneously. It should come as no surprise that the supply and demand for calcium is highly regulated. In evolution theory, the common dogma maintains that out of simple cells complex integrated systems emerged. Teleologically one could then argue that structures such as the calcium regulating parathyroid gland are critical in the physiological hierarchy. This is demonstrated in practical terms by noting that in humans small (20-50 micromolar) changes in serum calcium can elicit symptoms and signs of cardiac arrythmias and aberrant nerve conduction. Millimolar changes in serum calcium concentrations are fatal [51]. The parathyroids are charged with maintaining serum calcium levels within a physiologically safe range.

In most people, there are four parathyroid glands attached to a thyroid gland that can be found in the neck. Their size is approximately 7mm x 3mm x .5mm (Figure 1.1). The glands secrete a hormone inspirationally named parathyroid hormone (PTH). PTH is a peptide hormone that controls the level of ionized calcium in the blood and extra-cellular fluids. PTH binds to cell membrane receptors in bone, intestine and kidney and triggers responses that increase blood calcium. The increase blood calcium feeds back on the parathyroid gland by diffusing back to the PTH producing cells (chief cells) [51]. If the calcium concentration sensed by the cells is high enough, the cells do not secrete PTH (Figure 1.2).

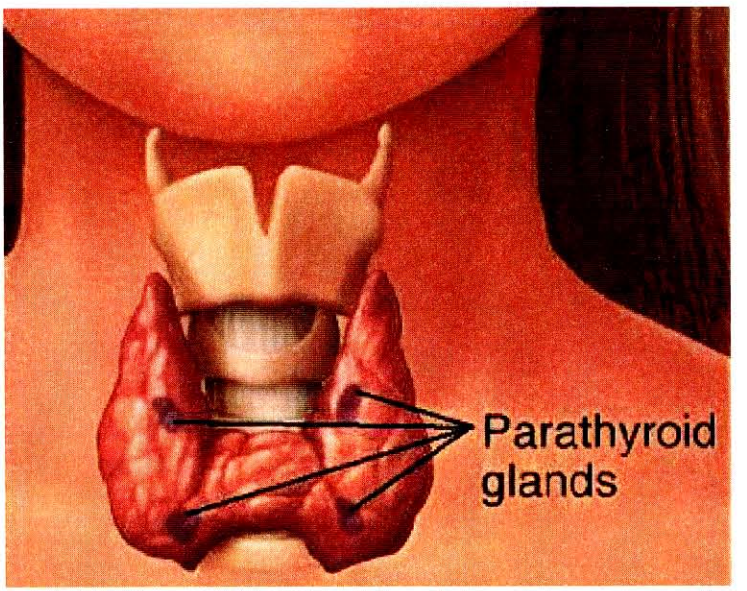

Figure 1.1: The parathyroid glands.

1.1.2 The physiological phenomena to be studied

Clinical and basic science researchers studying the parathyroid gland have established a general correlation of serum calcium levels to PTH release [16, 15, 38]. In the past decade great progress was made in the molecular biology of the parathyroid cells. For example, the calcium sensing receptor on parathyroid hormone secreting cells was cloned and specific receptor defects were identified in parathyroid pathologies [22, 18, 25]. As advancing and important as the molecular biology results have been, they at once shed light on the significant gap between our grasp on biochemistry and cell biology compared with our understanding of the whole gland macrophysiology.

On a macrophysiological scale PTH is normally observed to have an episodic secretory pattern. The episodes have a variable frequency, but in general occur 5-6 times per hour [16, 17, 38]. Their amplitude is approximately 25% above the baseline. The etiology of the periodic pattern is unknown. It has been shown that absolute levels of serum calcium do affect the level of PTH concentration on a long time scale (hours to days). However, clinical researchers have not observed changes in calcium concentration over the period of a typical PTH episode. The conclusion drawn from these results is that the episodic PTH pattern is not under the minute to minute influence

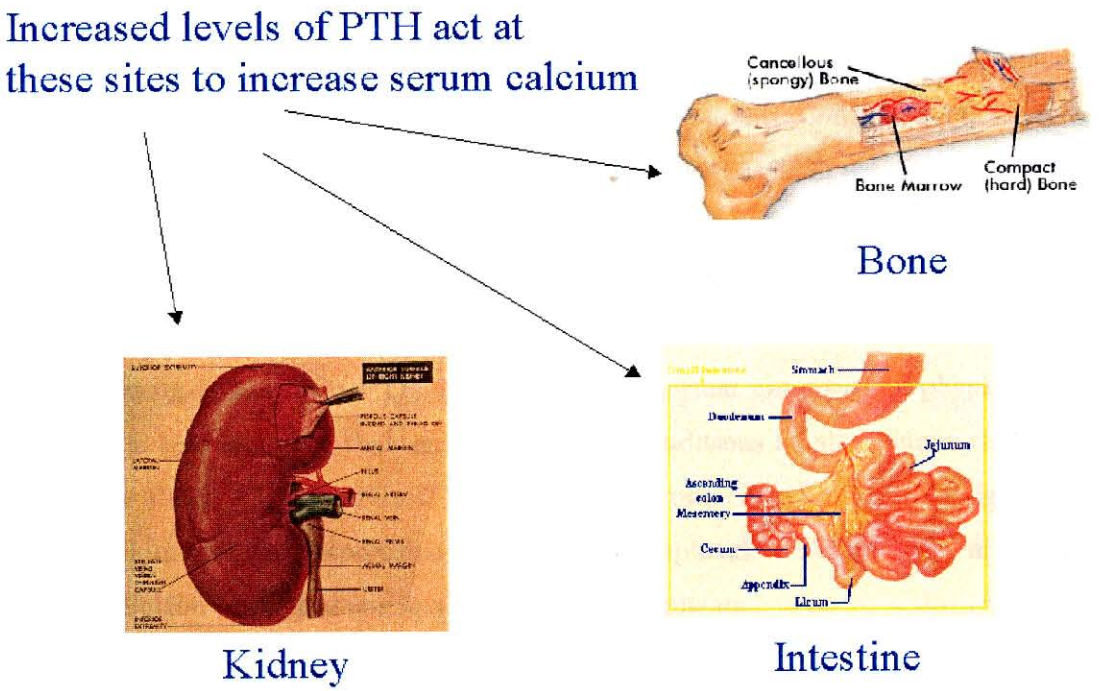

Figure 1.2: Target tissues of PTH.

of calcium concentration in the blood. Controlled infusion or "clamp" studies have also been used to examine the PTH physiological response to changing calcium concentrations [15, 3]. In these studies the level of calcium is controlled by either infusing a solution of calcium gluconate to increase blood calcium or by infusing sodium citrate to decrease calcium. The blood levels of calcium are monitored every minute to ensure the target calcium concentration. Within several minutes, a decrease in serum calcium of 0.2 mmol (5% change) can increase the serum PTH concentration by tenfold (1000%)[38]. The transient response settles after 20 minutes and if the calcium clamp is maintained at the new lower concentration, the PTH concentration remains elevated approximately two times above baseline; see Figure 1.3. **Thus it seems that the literature on PTH secretion contains a contradiction.** As just described, PTH has been shown to be exquisitely sensitive to small serum changes in calcium concentration in "clamp" experiments. How then could one argue for the uncorrelated calcium-PTH dynamics in the normal unperturbed physiological state, while also claiming that under controlled conditions small calcium changes caused very sharp PTH responses? The hypothesis offered in this work suggests that the calcium changes responsible for the small amplitude PTH episodes are beyond the resolution of clinical calcium measuring instruments.

Clinical clamp studies also show clear differences in the PTH response between subjects with definable pathologies and healthy controls [17, 15]. For example, the suppression of PTH secretion in patients with a PTH tumor (adenoma) is blunted when compared to the response in healthy subjects. Patients with adenoma and a similar entity called hyperplasia typically have PTH levels 10-20 times normal. There are also genetic diseases that alter PTH secretion. Familial hypocalciuric hypercalcemia (FHH) is an entity in which patients have receptor defects and elevated PTH, but unlike adenoma, high PTH levels in subjects with FHH can be inhibited by calcium infusion as easily as healthy subjects. An interesting observation seen regularly in the clamp experiments is that the rise time of the PTH curve induced by calcium lowering is consistently faster than the PTH decay time of calcium raising. This can be seen graphically by referring to Figure 5.12 in chapter 5. No explanation for this has been

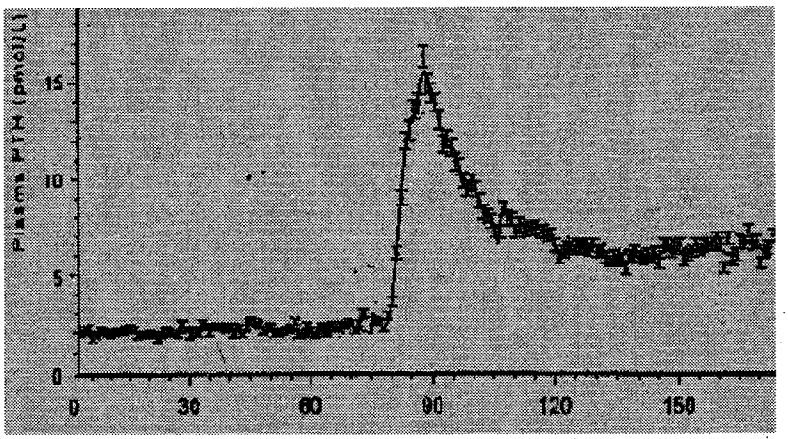

Figure 1.3: In the figure above, the Y-axis depicts PTH and the X-axis is time. At minute 75 blood calcium levels are lowered by means of introducing sodium citrate into the circulation. The rapid PTH rise is typical of healthy subjects.

given [39].

In summary, the basic macro-physiological phenomena to be addressed are as follows:

(a) The rapid and strong increase (decrease) in PTH secretion in response to moderately small changes in calcium concentration (using a controlled infusion).

(b) The blunted response to calcium infusion seen in a PTH secreting tumor or adenoma.

(c) The shifted response seen in the genetic disease familial hypocalciuric hypercalcemia (FHH).

(d) The poor correlation between minute-minute calcium changes and PTH concentration measured in the serum.

(e) The mechanism or etiology of the PTH episodes.

(f) The asymmetry in the rise and decay time of the PTH concentration in calcium infusion studies.

1.2 Synopsis of the cell-level physiology

1.2.1 Cell physiology background

Calcium and other molecules arrive to the gland and diffuse through capillaries and the inter-cellular spaces to eventually interact with chief cells (the PTH secreting cells). Chief cells sense changes in their extracellular environment by means of a calcium sensing receptor (Casr) that is described in some detail in the supplementary material. The binding of calcium to the sensor inhibits PTH secretion from its stored intracellular vesicles into the extracellular space. If the calcium concentration is below the level required for inhibition, the cell will secrete PTH. This process is called exocytosis. Once the PTH molecule is secreted, it diffuses in the intercellular spaces and eventually into the capillaries that carry it to the rest of the body (Figure 1.4). The glandular architecture is segmented into chords or nests of cells surrounded by a capillary network (Figure 9.4). The apical portions of a typical chief cells face inwardly toward other chief cells while the basal portion is often positioned near a capillary [40, 48]. The cells have been reported to have an apical-lateral secretory polarity [49] (see Figure 1.5). Adenomatous or tumor cells are larger and possess an abundant cytoplasm compared with normal cells. The adenomas are organized in dense sheets that crowd adjacent normal cells. Other PTH pathologies exist as well. One of these is a genetic disease (FHH) [25] that impairs the Casr. A further discussion of these pathologies is given in the supplementary material.

1.2.2 Three important results from the cell-level physiology

It has been observed that under identical experimental conditions, a single isolated parathyroid cell will secrete less PTH than a cell residing in a cluster of cells [13, 44]. This phenomenon has also been observed in other endocrine systems including the pancreas and the pituitary. Furthermore, a denser collection of cells secretes more PTH per cell than a more sparsely populated group. This effect could not be accounted for by the conditioned media in which the experiments were performed; thus, ruling out that the effect was a chemical reaction to a secretory product by the cells themselves. Yu et al. [54] reported the following intriguing result. A tissue sample

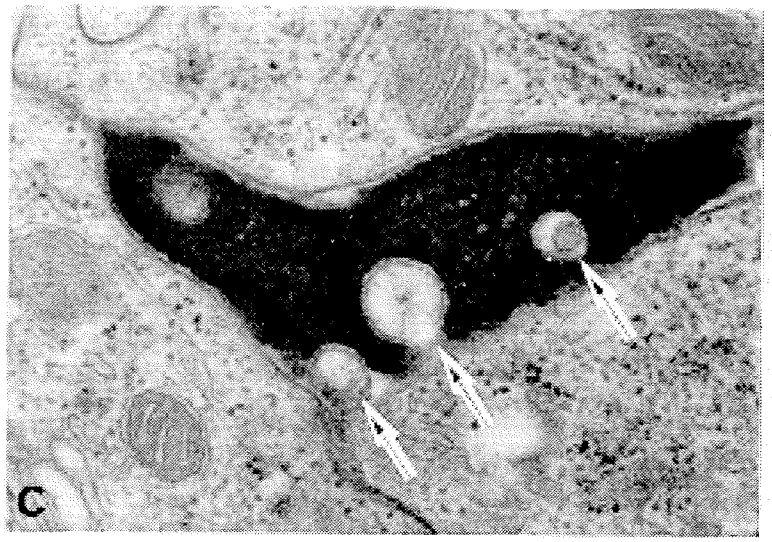

Figure 1.4: A storage vesicle is seen emptying its contents into the intercellular space.

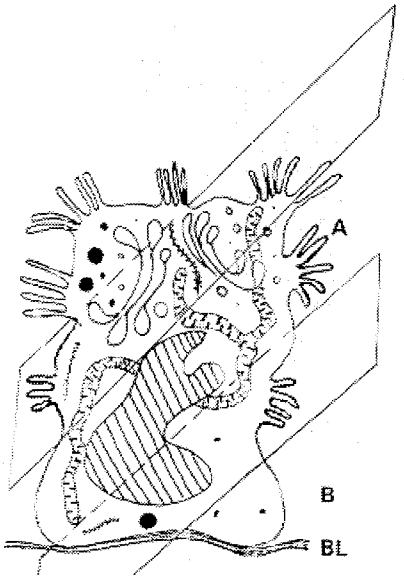

Figure 1.5: The PTH secreting cell possess an apical lateral polarity.

of cells from a PTH secreting tumor (adenoma) was studied for its ability to resist calcium suppression. The cells continued to secrete PTH in the presence of a calcium concentration that would normally suppress normal cells. The tumor cells were then fragmented into much smaller cell collections after which their PTH secretion was suppressed by the same calcium concentration that was previously ineffective. Together, these results help formulate a basis for our model which posits that diffusional transport of calcium plays a far more important role in PTH regulation than has previously been appreciated.

In summary, the three important cell level phenomena to be addressed are as follows:

(a) Single cells in isolation secrete less PTH per cell than cells residing in a cluster or group.

(b) Denser collections of cells secrete more than sparser collections.

(c) Adenomas are resistant to calcium suppression but can recover their sensitivity to calcium when they are dispersed.

Chapter 2 Hypothesis and Cell-Level Model

2.1 Philosophy

We are presented with a collection of experimental observations that in general fall into three categories.

(a) **Clinical research data from infusion tests**

(b) **In vitro studies on PTH secreting cells**

(c) **Observations from cell, biochemical and molecular biology experiments**

Ideally, our theory should be consistent with the observations on all these scales. The approach that is taken in this work is to attempt to minimize assumptions and simplify the physiology without discarding essential features. There is no doubt that any simplification of the full physiological phenomena is only an approximation and will consequently lack some measure of detail. However, that will not detract from the advantages gained by being able to wrap up a collection of seemingly disconnected and disparate phenomena into a unified principle.

We now proceed to the hypothesis and then the cell-level model.

2.2 Hypothesis: Diffusive transport of calcium mediates PTH secretion and PTH secretion modifies the calcium diffusivity.

Theoretical scenario of a PTH episode or pulse

It is reasonable to assume that a small decrement [1] in the calcium concentration near an individual cell initiates the release of that cells PTH and other co-stored proteins into an inter-cellular space shared by neighboring cells. The presence of large proteins in the extracellular matrix could increase the path length of a calcium molecule's transport to a target receptor, thus resulting in a decreased effective calcium diffusion. The arrival of fewer calcium ions promotes even more PTH release and ignites a runaway reaction of PTH secretion within the local nest or chord of cells. The secretory response is perhaps modulated by countering forces such as a rising calcium concentration and depletion of PTH from stored vesicles [39, 40]. In this configuration, the cell network is poised to tune its own secretory response by locally controlling molecular diffusion. There are two compelling consequences of this theory. One is that the PTH response could be the result of calcium concentration changes below clinical resolution. The second is that altered geometry and functionally ineffective calcium sensing receptors could establish a higher intercellular PTH concentration and dampen the regulatory effects of calcium, as is observed in vivo and in vitro studies of adenomas [15, 54].

Stated another way, the diffusive transport of calcium ions in the gland controls the PTH secretion and in turn the PTH secretion can alter the glandular diffusive transport of calcium. A cursory review of the described PTH secretory phenomena reveals the consistency of the hypothesis. The fact that the Casr is likely situated in the regions of exocytosis further supports this idea.

[1] smaller than can be measured by standard clinical electrodes

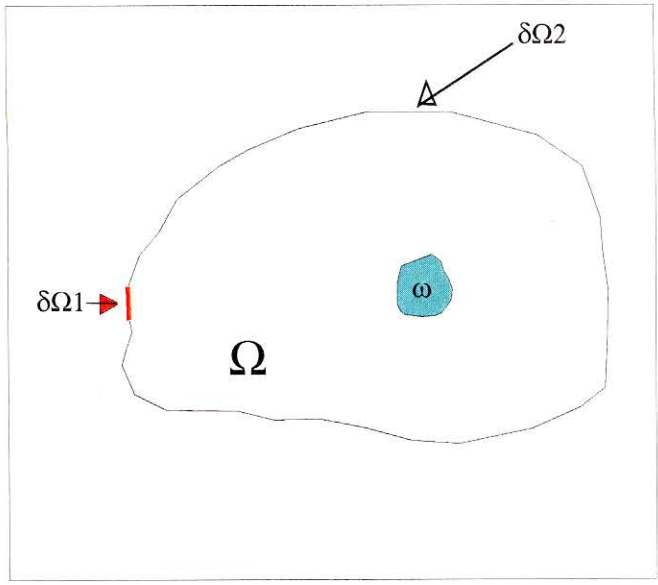

Figure 2.1: The cell level system of differential equations are solved on the domain Ω and the boundary conditions hold on $\partial\Omega$.The cell is represented by ω.

2.3 A cellular level model

The equations for the cell-level model are given below. The model assumptions and their justification follow. For reference a schematic diagram Figure 6.3 illustrates the relationship between the cell-level and glandular modeling domains.

2.3.1 The cell-level equations

Consider a domain Ω consisting of interstitial fluid plus a single cell ω; see Figure 2.1. Assume that diffusion is the only important transport mechanism. Then, we assume that the extracellular calcium concentration $C^*(\mathbf{x}^*, t^*)$ and the extracellular PTH concentration $P^*(\mathbf{x}^*, t^*)$ evolve according to

$$\frac{\partial C^*}{\partial t^*} = \nabla \cdot (D^*(P^*)\ \nabla C^*), \tag{2.1}$$

$$\frac{\partial P^*}{\partial t^*} = \nabla \cdot (D_{p^*}\ \nabla P^*) + \chi(\mathbf{x}^*)\mathcal{S}^*, \tag{2.2}$$

$$\text{for } \mathbf{x}^* \in \Omega, t^* > 0.$$

where

$$\chi(\mathbf{x}^*) = \begin{cases} 1 \; if \; \mathbf{x}^* \in \omega \\ 0 \; if \; \mathbf{x}^* \notin \omega, \end{cases} \tag{2.3}$$

so that the source S^* is confined to the cell.

The effect of PTH on calcium diffusion is through the diffusivity $D^*(P^*)$, which we take as

$$D^*(P^*) = D_{c^*} \exp(-\lambda^* P^*), \tag{2.4}$$

where D_{c^*} is the calcium diffusivity in physiological serum. The source S^* for PTH depends on the calcium concentration C^* and the amount $I(\mathbf{x}^*, t^*)$ of stored PTH, in intracellular vesicles, that is released into the extracellular domain. We take

$$\mathcal{S}^*(C^*, I^*) = \alpha^* \; (C^*_{cell} - C^*(\mathbf{x}^*, t^*)) I^*(\mathbf{x}^*, t^*) H(C^*_{cell} - C^*(\mathbf{x}^*, t^*)), \tag{2.5}$$

where

$$H(C^*_{cell} - C^*) = \begin{cases} 1 \; if \; C^* < C^*_{cell} \\ 0 \; if \; C^* \geq C^*_{cell}, \end{cases} \tag{2.6}$$

and where

$$\frac{\partial I^*}{\partial t^*} = \kappa^* V^* - S^*(C^*, I^*). \tag{2.7}$$

$$\mathbf{x}^* \in \omega, \mathbf{t}^* > \mathbf{0}.$$

Thus, as implied by the Heaviside function H, PTH is released only when the concentration C^* is less than some threshold level C^*_{cell}, and since $\mathbf{x}^* \in \omega$ for (2.7), the evolution of I^* is confined to the cell.

In equations $\lambda^*, \alpha^*, \kappa^*$ are necessary dimensional constants we account for later when we introduce dimensionless variables. V^* represents the constant production of intracellular PTH contained in vesicles. We take D^*_p and D_{c^*} the diffusivity in the serum, of PTH and calcium respectively, to be constant.

The boundary $\delta\Omega$ of Ω is composed of two parts, $\delta\Omega_1$ and $\delta\Omega_2$ (see Figure 2.1), so that $\partial\Omega = \delta\Omega_1 \cup \delta\Omega_2$. Our initial and boundary conditions are

$$\frac{\partial P^*}{\partial n} \equiv \nabla P^*.\hat{\mathbf{n}} = 0 \quad on \quad \partial\Omega \tag{2.8}$$

$$\frac{\partial C^*}{\partial n} \equiv \nabla C^*.\hat{\mathbf{n}} = 0 \quad on \quad \delta\Omega_2 \tag{2.9}$$

$$C^*(\mathbf{x}, t) = \widehat{C^*} \quad on \quad \delta\Omega_1 \tag{2.10}$$

where $\hat{\mathbf{n}}$ is the unit outward normal to the boundary of $\partial\,\Omega$. The initial conditions are

$$P^*(\mathbf{x}, t = 0) = 0, \tag{2.11}$$

$$I^*(\mathbf{x}, t = 0) = I^*_0, \tag{2.12}$$

$$C^*(\mathbf{x}, t = 0) = C^*_0 \leq C^*_{cell}. \tag{2.13}$$

Here $\widehat{C^*}, C^*_0, I^*_0$ are constants. To be consistent with our later glandular model (chapter 4), we are introducing calcium into the interstium only on a small segment of the boundary.

It is convenient to introduce dimensionless variables into the above equations as follows. We scale our spatial coordinates by L, the length of a typical cell ω in the cell-model, and we scale time by the diffusion time $\tau = L^2/D_{c^*}$. The scaled time and coordinates then become $t = t^*/\tau$ and $x = \mathbf{x}^*/L$. The calcium, PTH and intracellular PTH concentrations are scaled by a reference calcium value and reference PTH values denoted by C_r, P_r and I_r respectively. Let $C = C^*/C_r$, $P = P^*/P_r$, $I = I^*/I_r$,

$V = V^*/I_r$, $C_{cell} = C^*_{cell}/C_r$, $I_0 = I^*_0/I_r$, $C_0 = C^*_0/C_r$, $\widehat{C} = \widehat{C}^*/C_r$.

Rewriting the above calcium, PTH and Intracellular PTH equations in these scaled coordinates, we get the dimensionless system of equations.

$$\begin{aligned}
\frac{\partial C}{\partial t} &= \nabla \cdot (\exp^{-\lambda P} \ \nabla C), && \mathrm{x} \in \Omega, t > 0, \\
\frac{\partial P}{\partial t} &= \nabla \cdot (D_p \ \nabla P) + \chi(x) S(C, I), && \mathrm{x} \in \Omega, t > 0, \\
\frac{\partial I}{\partial t} &= \kappa V - S(C, I), && \mathrm{x} \in \omega, t > 0,
\end{aligned} \tag{2.14}$$

where

$$S(C, I) = \alpha\{C_{cell} - C(\mathbf{x}, t)\} I(x, t) H(C_{cell} - C), \tag{2.15}$$

and where

$$\kappa = \frac{\kappa^* L^2}{D_{c^*}}, \tag{2.16}$$

$$D_p = D_{p^*}/D_{c^*}, \tag{2.17}$$

$$\alpha = \frac{\alpha^* L^2 C_r}{D_{c^*}}, \tag{2.18}$$

$$\lambda = \lambda^* P_r, \tag{2.19}$$

and

λ^*= the scaling factor (in units of $1/PTH$) for calcium diffusivity dependence on PTH,

κ^*= the rate of production of vesicularly stored PTH,

α^*= the rate of exocytosis of intracellular PTH,

D_{c^*}= the diffusivity of serum calcium,

D_{p^*}= the diffusivity of serum PTH,

C^*_{cell}= the calcium threshold level for exocytosis.

The constants κ^*,V^*,λ^*,$C^*_{cell}, D_{c^*}, D_{p^*}, \alpha^*$ are all ≥ 0.

It is important to note that in this model, source $S(C, I)$ is confined to the cell region ω.

Our dimensionless boundary conditions are

$$\frac{\partial C}{\partial n} \equiv \nabla C.\hat{\mathbf{n}} = 0 \ on \ \delta\Omega_2, \tag{2.20}$$

$$\frac{\partial P}{\partial n} \equiv \nabla P.\hat{\mathbf{n}} = 0 \ on \ \delta\Omega, \tag{2.21}$$

$$C(\mathbf{x}, t) = \widehat{C} \ on \ \delta\Omega_1, \tag{2.22}$$

where $\hat{\mathbf{n}}$ is the unit outward normal to the boundary of $\partial\,\Omega$. $\widehat{C}$ is in general a constant. The initial conditions in dimensionless form now become

$$P(\mathbf{x}, t = 0) = 0, \tag{2.23}$$

$$I(\mathbf{x}, t = 0) = I_0, \tag{2.24}$$

$$C(\mathbf{x}, t = 0) = C_0 \leq C_{cell}. \tag{2.25}$$

Assumptions and Jusifications

(a) We use a 2-d model in the cell-level simulations since chief cells can be thought of as pancake like in geometry.$(x^*, y^*) = (\mathbf{x}^*) \in \mathbf{\Omega}$.

(b) Interstitial transport of calcium and PTH occurs by diffusion. Our regulatory hypothesis rests upon the factors modifying diffusion [7, 8, 11, 14, 50, 52, ?]. The diffusion of small ions in a polymeric solution has been the subject of several papers in the literature [26, 31, 23, 34, 27, 28, 29]. The diffusion coefficient D is affected by the fraction of the diffusible volume occupied by larger proteins (PTH, chromogranin A). There are no studies concerning the diffusion of calcium

in the parathyroid gland. Yam et al. [52], using an empirical formula, published a study comparing the diffusion of small ions (calcium and sodium) in polymeric solutions. The formula employed was $D = D_o \exp(-\alpha M^{\nu})$ where D_0 is the free diffusion coefficient, M is protein concentration, and α, ν are constants. This motivates equation 2.3. We have chosen to keep the diffusivity of PTH constant at this time.

(c) The cells have calcium sensing receptors. We assume that the calcium occupancy of the receptors is proportional to the concentration of calcium in a small neighborhood of the receptor's extracellular domain. In the simple cell model level, we assume that the cell receptor and exocytosis sites are the same. The justification for this comes from a study by Kifor et al. [22]. In that study the calcium sensor was found to be localized in caveolin-rich domains. Caveolin has been associated with exocytotic locations on the cell membranes surfaces [22, 1].

(d) We assign an empirical rule for PTH release. There is ample evidence suggesting that ambient calcium concentration and cell PTH release are related [51]. In the model, the receptor has a given "calcium threshold;" below which PTH is released, and above which PTH exocytosis is inhibited. We justify this assumption by referring to studies in the literature characterizing calcium-PTH response curves with set points and thresholds [13, 44]. Furthermore, the quantity of PTH released is dependent on the available intracellular PTH stores [21].

(e) Intracellular PTH dynamics. PTH release is modified by available cellular stores of ("I"). We use a differential equation to dynamically update the state of each cell receptor/release site in the simulation.

To briefly summarize:

- Calcium ions diffuse in the intercellular spaces. Its diffusivity depends on the domain geometry and PTH concentration.
- PTH is released if the extracellular calcium concentration at the receptor site is below the cell's calcium threshold.
- The amount of PTH released is modified depending upon the availability of intra-cellular PTH stores.

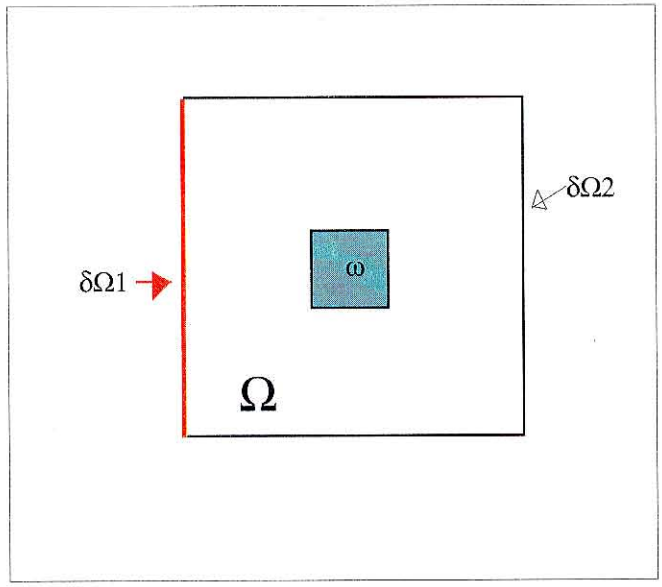

Figure 2.2: The cell level system of differential equations are numerically solved on the domain Ω and the boundary conditions hold on $\partial\Omega$. The cell is represented by ω.

Cell-level model numerical details

The above coupled PDEs (equations 2.14) are solved numerically using finite differences. Figure 2.2 depicts our computational domain. We first define a Cartesian domain. This domain is discretized with a uniform mesh of $N \times M$ with N (resp. M) points in the x (resp. y) direction. Points on this mesh are indexed by (i, j) such that $i = 1, 2, \cdots, N$ and $j = 1, 2, \cdots M$.

The spatial derivatives are computed using centered 2nd order finite differences. We update the concentrations of calcium and PTH by explicit time-marching using a 2nd order Runge-Kutta time integration scheme. The diffusion terms are discretized using 2nd order central differences as

$$\begin{aligned} \nabla \cdot (D_c \, \nabla C)_{i,j} \quad = \quad & D_{c,i,j} \frac{C_{i+1,j} + C_{i-1,j} + C_{i,j+1} + C_{i,j-1} - 4C_{i,j}}{\Delta^2} + \\ & \frac{(D_{c,i+1,j} - D_{c,i-1,j})(C_{i+1,j} - C_{i-1,j})}{4\Delta^2} + \\ & \frac{(D_{c,i,j+1} - D_{c,i,j-1})(C_{i,j+1} - C_{i,j-1})}{4\Delta^2}. \end{aligned} \tag{2.26}$$

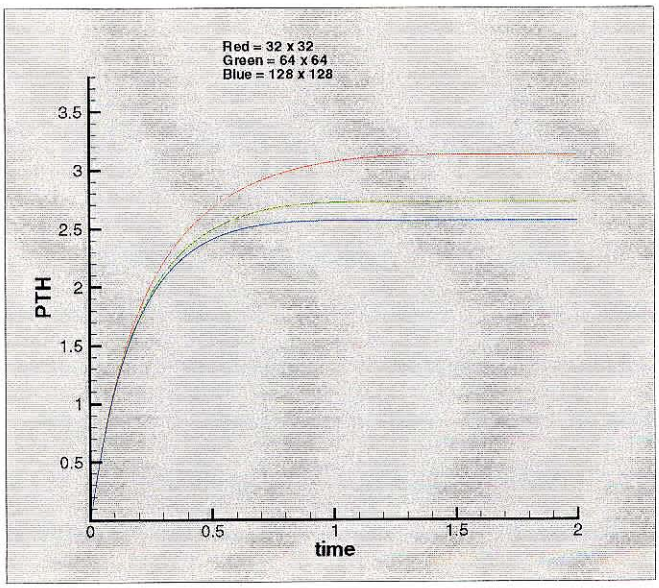

Figure 2.3: These curves represent the same "test" protocol at increasing resolution of the mesh as discussed in the text.

The Neumann boundary conditions are calculated using 2nd order one sided differencing. For the left boundary of $\delta\Omega$ the condition for P would be

$$P_{i,j} = \frac{4}{3}P_{i+1,j} - \frac{1}{3}P_{i+2,j}. \tag{2.27}$$

We represent the cell ω as a small square inside our square shaped interstitial domain Ω. The values used for initial conditions, boundary conditions and parameters are listed below.

The model's convergence properties were evaluated by testing a known PTH calcium infusion algorithm at progressively finer mesh resolution n x m, 2n x 2m, 4n x 4m. Where n=32 and m=32, Figure 2.3 graphically displays quadratic convergence which is expected from the 2nd order finite difference scheme.

Parameter	Value
α	8.00
V	1.0
κ	0.10
λ	1.00
I_0	0.40
C_0	0.95
$\widehat{C}$	1.10
C_{cell}	1.00

Table 2.1: A list of the parameters and the values used in general.

Chapter 3 Computational Experiments

In this section we will examine the model's ability to capture the cellular-level PTH secretory phenomena that we again list below. The larger objective is to demonstrate that the secretory phenomena arising from diffusion dependent PTH regulation at the cell level are related to the secretory phenomena seen at the glandular level. The goal is certainly not to capture the detail of the cell machinery, but rather the essential relationship between transport, spacing and hormonal release.

The key experimental observations are as follows:

(a) Single cells in isolation secrete less PTH per cell than cells residing in a cluster or group.

(b) Denser collections of cells secrete more than sparser collections.

(c) Adenomas are resistant to calcium suppression but can recover their sensitivity to calcium when they are dispersed. In addition adenomas secrete more PTH per cell than do normal cells.

3.1 Single isolated cell vs group of cells

The simulation is set up to mimic an in vitro experiment that will measure the PTH output of a single isolated cell and then compare the result with a simulation using a group of cells. We start the simulation by initially stimulating the cell (or cells) with a calcium concentration below the inhibitory threshold and then suppress the PTH output by enforcing our boundary conditions given below.

We enforce a zero-flux boundary condition for P and C on all the boundaries of Ω except a Dirichlet condition on the left boundary for C.

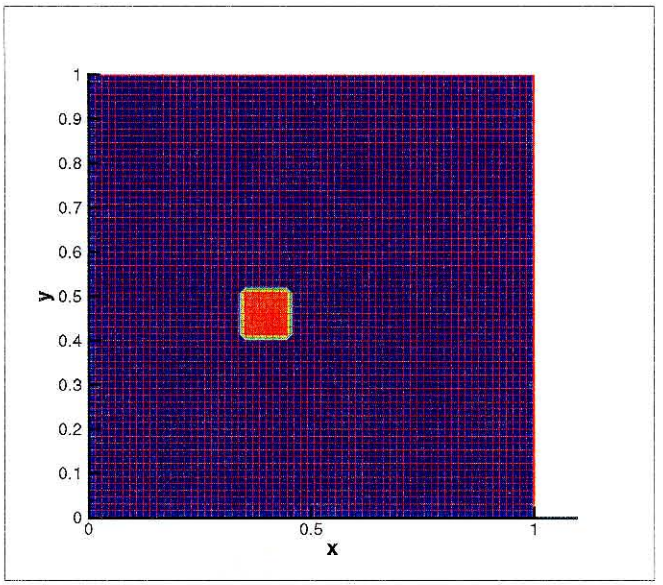

Figure 3.1: This figure shows the region of our single isolated cell. The PTH response of this cell is compared to the response of two and four cells in Figure 3.3.

$$\frac{\partial C}{\partial n} \equiv \nabla(C).\hat{\mathbf{n}} = 0, \mathbf{x} \in \mathbf{\Omega} \tag{3.1}$$

$$\frac{\partial P}{\partial n} \equiv \nabla(P).\hat{\mathbf{n}} = 0, \mathbf{x} \in \mathbf{\Omega} \tag{3.2}$$

$$C(\mathbf{x}, t) = \widehat{C} \ \ on \ \ \delta\Omega_1 \tag{3.3}$$

where $\widehat{C} > C_{cell}$

The parameters used in these simulations are the following unless stated otherwise.

$$\widehat{C} = 1.1, \kappa = 0.1, \lambda = 1, \alpha = 8.0, C_{cell} = 1.0, D_p = 1.0. \tag{3.4}$$

Figure 3.1 and Figure 3.2 show the location of the single cell and group of four cells with respect to the $\delta\Omega_1$. It should be noted that the group of four cells is placed closer to $\delta\Omega_1$ than the single isolated cell. Had the placement of the four cells been simply to extend the four-cell region equally in all directions, the area furthest from the left boundary would produce more PTH than areas more proximal to the left boundary.

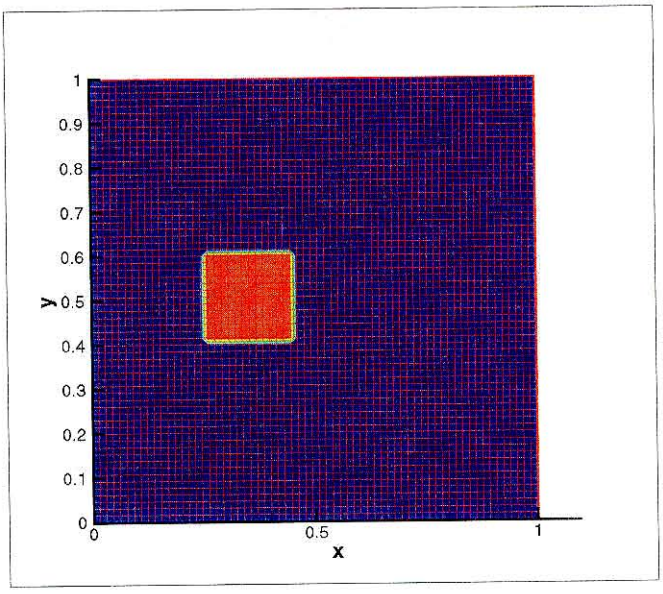

Figure 3.2: This figure shows a region that represents four cells.

Thus in order not to bias the simulation in favor of the group, the group of four cells is placed closer to the left boundary. In addition, we conducted a simulation comparing two cells and the single isolated cell. The results of the four cells, two cells and single cell are shown in Figure 3.3.

These simulations show the consistency of the model behavior with the corresponding experimental literature on PTH secretion in single vs groups of cells [13]. If the group response were a linear sum of individual single cells, the total for the group of four would simply be four times the value of a single cell(0.05), which would be 0.20 in this case. Less dramatic is the simulation of two cells compared to the isolated single cell. However, it is still the case that the linear sum two isolated cells is less than the two connected cells which is 0.11 in this simulation. The effects of PTH concentration on the calcium diffusivity results in a nonlinear increase of PTH secretion for the cells residing in a group.

3.2 Density effects

In a sense we have already resolved this question in the previous simulations. It is anticipated that if two identical cells are spaced far enough apart from each other

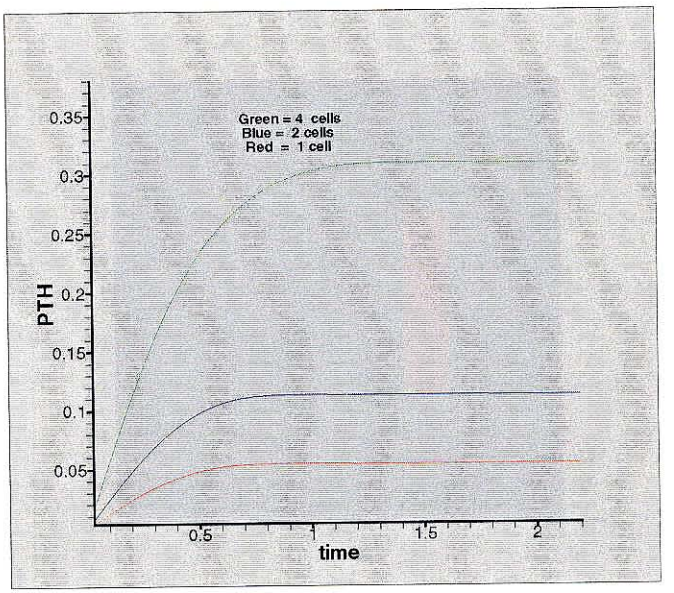

Figure 3.3: The top, middle and bottom curves represent the PTH response of four cells = 0.3, two cells = .11 and a single cell = 0.05 respectively.

and equidistant from a common source of calcium, they would behave individually as isolated cells. Whereas the same cells positioned in closer together will exhibit the nonlinear effects seen in the simulation of the group of cells. Here we consider two groups of two cells. Their positions are shown in Figure 3.4 and Figure 3.5. The PTH response for these two cases are depicted in Figure 3.6. As seen in the figure, the sparser set of cells collectively produce less PTH than the denser collection.

The first two computational experiments combined are consistent with the two experimental results of Sun et al., which demonstrated the single cell vs group effects as well as the cell crowding effects.

3.3 Adenomas and calcium resistance

In the introductory background, we described the experimental results of Yu et al. [54]. The authors in that study noted that an intact tissue sample from an adenoma was resistant (continued to secrete PTH) to calcium concentrations that are inhibitory for healthy cells. However, the very same tumor cells were inhibited by the identical calcium concentration after the tissue sample had been separated into smaller frag-

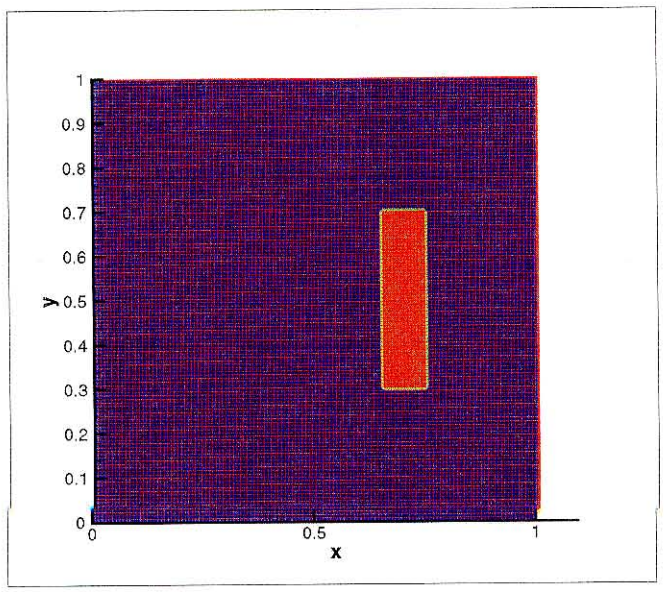

[!t]

Figure 3.4: Here we depict a region of four cells.

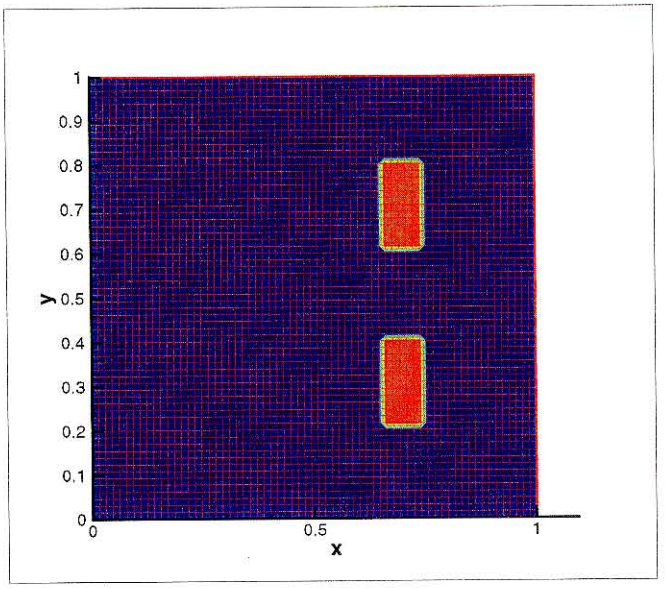

Figure 3.5: Here we display two regions (composed of two cells each) spaced far apart.

ments of cells. In our simulation of this experiment, we employ the same protocol as we have described for the previous simulations. We consider a region of "9 x 9" cells as our adenoma (Figure 3.7). We then fragment the tumor into nine separate cells and once again ensure the validity of the simulation by positioning the fragmented cells farther from the left boundary than the adenoma (Figure 3.8). The PTH secretory

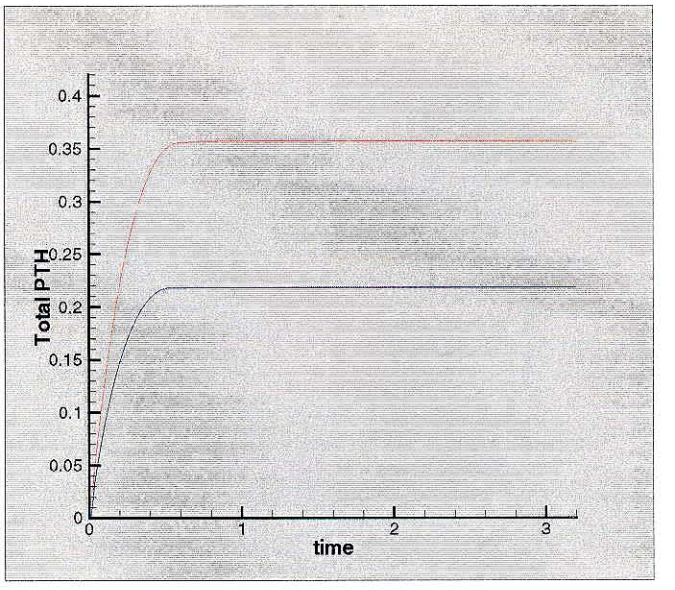

Figure 3.6: The upper curve shows the increased PTH secretion when the two, two-cell regions are close. The lower curve shows the PTH response when the regions are spaced farther apart.

response for these two cases are shown in Figure 3.9. The adenoma as a connected group of cells clearly secretes more PTH than its individual cells or fragments. This is consistent with the result reported in Yu et al. In Figure 3.10 the effect of the adenoma on calcium diffusion is shown. Note the slowing of the calcium in the region of active hormone secretion. We will show a parallel result in a glandular-level simulation of an adenoma.

3.4 Summary of the simple-cell model

The model was able to display the three in vitro cell-level phenomena as a consequence of the nonlinear diffusivity of calcium. Higher PTH concentrations slow the calcium transport and create a "resistive" state in regions with both greater numbers of cells and more densely spaced cell populations. Viewed through the assumption of PTH dependence in calcium's diffusivity, the three cell-level phenomena are just special cases of the same principle. We will now present a glandular level model that preserves the essential physiology seen here.

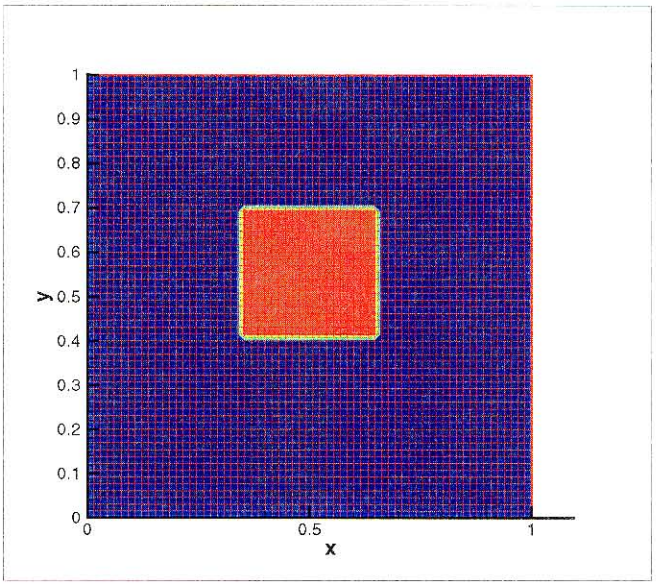

Figure 3.7: The intact adenoma which in this case is made up of nine cells.

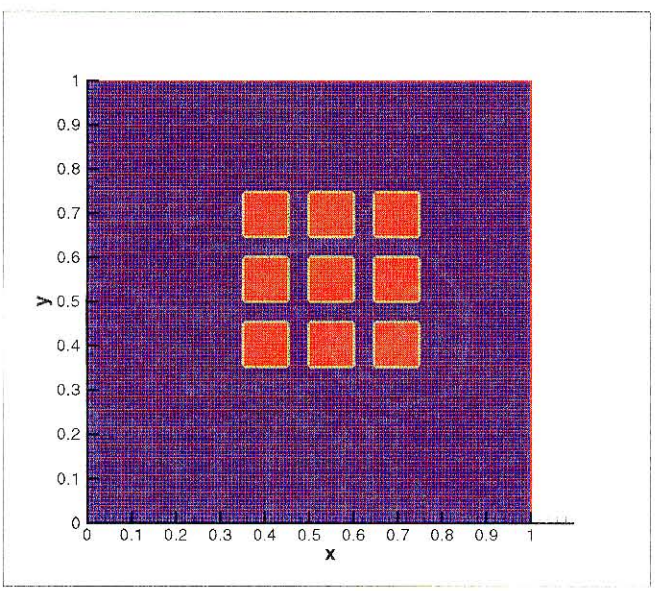

Figure 3.8: The nine adenoma cells are fragmented and spaced apart. Note that the fragments are positioned farther away from the Left boundary of Ω so as to not bias the PTH secretion in favor of the intact adenoma.

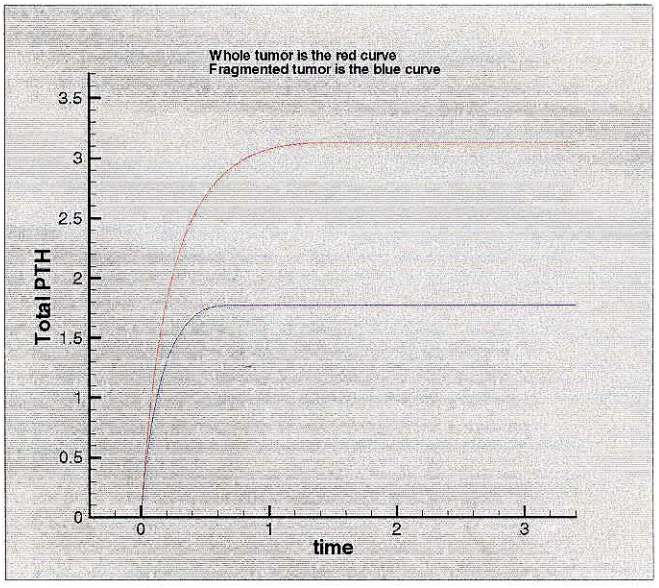

Figure 3.9: The intact adenoma secretes almost twice as much as the fragmented adenoma.

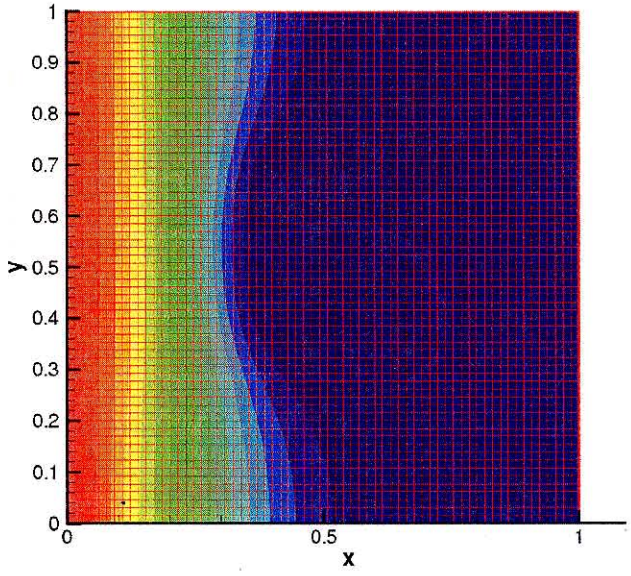

Figure 3.10: The calcium contours can be seen to "bend" as the diffusion of calcium slows down in the vicinity of a secreting adenoma.

Chapter 4 Glandular-level Model

In our attempt to model the physiology of the gland, we will have to sacrifice the spatial resolution of the simple cell model. Despite that we will show that the glandular level model will be able to demonstrate the important PTH secretory physiology. The model equations will now be introduced. The general form of the equations will be similar to the simple cell model with the exception of additional advection terms representing the carrying of blood to and from the gland.

4.1 Model construction

Our domain Ω, depicted by the schematic drawing Figure 4.1, consists of a parathyroid gland (and its PTH producing cells) along with the inflow and outflow blood vessels. In the gland itself, we assume the dominant transport of molecular species is diffusion while in the larger blood vessels entering and leaving the gland, the transport by advection is dominant. The left most boundary represents the inflow artery entering our gland, and the far right boundary is the outflow vein. We assume that blood plasma is conserved and that the flow of blood into the gland is steady. Let $\mathbf{u}^*$ represent the velocity field of the fluid (plasma) through the parathyroid gland. Then, we assume that the extracellular calcium concentration $C^*(\mathbf{x}^*, t^*)$ and the extracellular PTH concentration $P^*(\mathbf{x}^*, t^*)$ evolve according to

$$\frac{\partial C^*}{\partial t^*} + \mathbf{u}^* \cdot \nabla C^* = \nabla \cdot (D^*(P^*)\, \nabla C^*) \tag{4.1}$$

$$\frac{\partial P^*}{\partial t^*} + \mathbf{u}^* \cdot \nabla P^* = \nabla \cdot (D_{p^*}\, \nabla P^*) + \mathcal{S}^* \tag{4.2}$$

for $\mathbf{x}^* \in \Omega, t^* > 0$.

The effect of PTH on calcium diffusion is through the diffusivity $D^*(P^*)$, which we

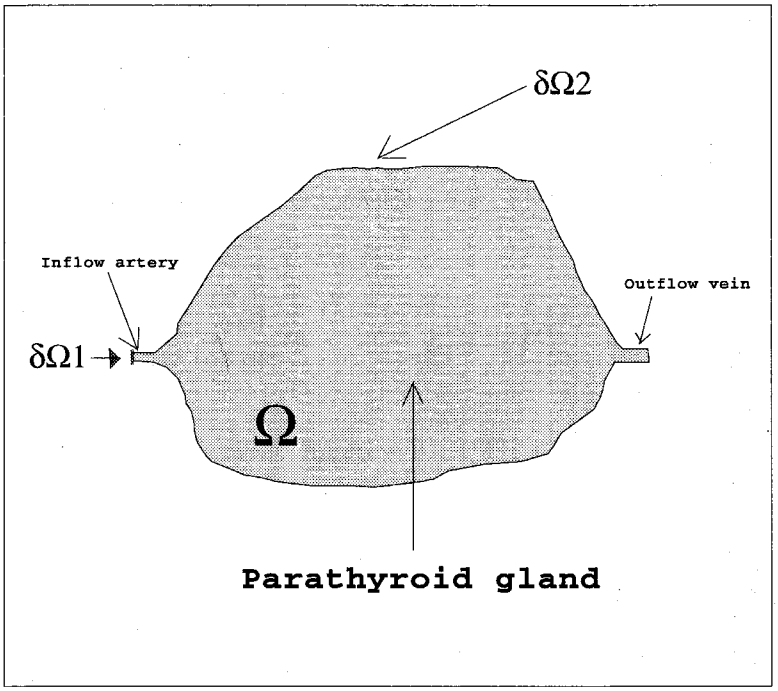

Figure 4.1: Our domain consists of the parathyroid gland and the incoming artery and outgoing vein.

take as

$$D^*(P^*) = \frac{D_{c^*} e^{-\lambda^* P^*}}{\rho(\mathbf{x}^*, t^*)}, \tag{4.3}$$

where D_{c^*} is the calcium diffusivity in physiological serum and $\rho(\mathbf{x}^*, t^*)$ is a dimensionless factor that represents the ratio of the gland density to that of a reference gland density.

The source S^* for PTH depends on the calcium concentration C^* and the amount $I(\mathbf{x}^*, t^*)$ of stored PTH, in intracellular vesicles, that is released into the extracellular domain. We take

$$\mathcal{S}^*(C^*, I^*) = \alpha^* \ (C^*_{cell} - C^*(\mathbf{x}^*, t^*))I^*(\mathbf{x}^*, t^*)H(C^*_{cell} - C^*(\mathbf{x}^*, t^*)), \tag{4.4}$$

where

$$H(C^*_{cell} - C^*) = \begin{cases} 1 \; if \; C^* < C^*_{cell} \\ 0 \; if \; C^* \geq C^*_{cell}, \end{cases}$$

and where

$$\frac{\partial I^*}{\partial t^*} = \kappa^* V^* - S^*(C^*, I^*). \tag{4.5}$$

Thus, implied by the Heaviside function H, PTH is released only when the concentration C^* is less than some threshold level C^*_{cell} as it was in the cell model. We implicitly assume that calcium ions and PTH (parathyroid hormone) are passively advected scalars by the fluid velocity. Furthermore, we assume that PTH is *generated* within the gland only and is absent in the blood flowing *into* the gland.

Analogous to the cell model, $\lambda^*, \alpha^*, \kappa^*$ are necessary dimensional constants we account for later when we introduce dimensionless variables. V^* represents the constant production of intracellular PTH contained in vesicles. We take D^*_p and D_{c^*}, the diffusivity in the serum of PTH and calcium respectively, to be constant.

The boundary $\partial\Omega$ of Ω is composed of two parts, $\delta\Omega_1$ and $\delta\Omega_2$ (see Figure 4.1), so that $\partial\Omega = \delta\Omega_1 \cup \delta\Omega_2$. Our initial and boundary conditions are

$$\frac{\partial C^*}{\partial n} \equiv \nabla C^*.\hat{\mathbf{n}} = 0 \; on \; \delta_2\Omega, \tag{4.6}$$

$$C^*(\mathbf{x}, t) = \widehat{C^*} \; on \; \delta_1\Omega, \tag{4.7}$$

$$\frac{\partial P^*}{\partial n} \equiv \nabla P^*.\hat{\mathbf{n}} = 0 \; on \; \partial\Omega, \tag{4.8}$$

where $\hat{\mathbf{n}}$ is the unit outward normal to the boundary of $\partial\,\Omega$. The initial conditions are

$$P^*(\mathbf{x}, t = 0) = 0, \tag{4.9}$$

$$I^*(\mathbf{x}, t = 0) = I^*_0, \tag{4.10}$$

$$C^*(\mathbf{x}, t = 0) = C^*_0 \leq C^*_{cell}. \tag{4.11}$$

Here $\widehat{C^*}, C_0^*, I_0^*$ are constants.

It is convenient to introduce dimensionless variables to the above as follows. We scale our spatial coordinates by L, the length of a typical gland, we scale time by the diffusion time $\tau = L^2/D_{c^*}$ and we scale velocity by U_0, the average incoming arterial velocity. The scaled time and coordinates then become $t = t^*/\tau$, $x = \mathbf{x}^*/L$ and $u = \mathbf{u}^*/U_0$. The calcium, extracellular PTH and intracellular PTH concentrations are scaled by a reference calcium value and reference extracellular and intracellular PTH values denoted by C_r, P_r and I_r respectively. Let $C = C^*/C_r$, $P = P^*/P_r$, $I = I^*/I_r$, $V = V^*/I_r$, $C_{cell} = C_{cell}^*/C_r$, $I_0 = I_0^*/I_r$, $C_0 = C_0^*/C_r$, $\widehat{C} = \widehat{C}^*/C_r$.

Rewriting the above calcium, PTH and intracellular PTH equations in these scaled coordinates, we get the dimensionless system of equations.

$$\begin{aligned}
\frac{\partial C}{\partial t} + Re\ Sc\ u \cdot \nabla C &= \nabla \cdot (\rho^{-1} e^{-\lambda P}\ \nabla C), && (4.12)\\
\frac{\partial P}{\partial t} + Re\ Sc\ u \cdot \nabla P &= \nabla \cdot (D_p\ \nabla P) + S(C, I), && (4.13)\\
\frac{\partial I}{\partial t} &= \kappa V - S(C, I), && (4.14)
\end{aligned}$$

where

$$S(C, I) = \alpha(C_{cell} - C(x, t))I(x, t)H(C_{cell} - C), \qquad (4.15)$$

and

$$\begin{aligned}
\kappa &= \frac{\kappa^* L^2}{D_{c^*}}, && (4.16)\\
D_p &= D_{p^*}/D_{c^*}, && (4.17)\\
\alpha &= \frac{\alpha^* L^2 C_r}{D_{c^*}}, && (4.18)\\
\lambda &= \lambda^* P_r. && (4.19)
\end{aligned}$$

An additional consequence of the above scaling is that we introduce two non-dimensional parameters not seen in the cell model: the Reynolds number, Re, and the Schmidt number, Sc, defined as

$$Re = \frac{U_0\ L}{\nu}, \quad Sc = \frac{\nu}{D_{c0}}, \tag{4.20}$$

where ν is the kinematic viscosity of the plasma. The Reynolds number represents the ratio of inertial to viscous forces in a fluid, and the Schmidt number is the ratio of viscous diffusion to mass diffusion. The dimensionless parameter ρ represents the ratio of the gland density to that of a reference density.

The model constants,

λ^*= the scaling factor (in units of $1/PTH$) for calcium diffusivity dependence on PTH,

κ^*= the rate of production of vesicularly stored PTH,

α^*= the rate of exocytosis of intracellular PTH,

D_{c^*}= the diffusivity of serum calcium,

D_{p^*}= the diffusivity of serum PTH,

C^*_{cell}= the calcium threshold level for exocytosis,

are all ≥ 0.

Our dimensionless boundary conditions are

$$\frac{\partial C}{\partial n} \equiv \nabla C.\hat{\mathbf{n}} = 0 \ \ on \ \ \delta\Omega_2, \tag{4.21}$$

$$C(\mathbf{x}, t) = \widehat{C} \ \ on \ \ \delta\Omega_2, \tag{4.22}$$

$$\frac{\partial P}{\partial n} \equiv \nabla P.\hat{\mathbf{n}} = 0 \ \ on \ \ \partial\Omega, \tag{4.23}$$

where $\hat{\mathbf{n}}$ is the unit outward normal to the boundary of $\partial\,\Omega$. $\widehat{C}$ is in general a constant. The initial conditions in dimensionless form now become

$$P(\mathbf{x}, t = 0) = 0, \tag{4.24}$$

$$I(\mathbf{x}, t = 0) = I_0, \tag{4.25}$$

$$C(\mathbf{x}, t = 0) = C_0 \leq C_{cell}. \tag{4.26}$$

Justifications for the glandular-level model

The model equations in both the cell and glandular simulations are essentially the same, with two exceptions. The $\chi(x)I(\mathbf{x}^*, t^*)$ is now $I(\mathbf{x}^*, t^*)$ and there is an advection term in the glandular model. The advection term is dominant only in the vasculature entering the gland and is negligible in the glandular interstitium.

(a) We use a 2-d model in all simulations. Each parathyroid gland is on average 7mm x 3mm x 0.5 mm and therefore we feel that the aspect ratio justifies the 2-d approximation for a first model.[51]

(b) We assume $\mathbf{u} = (\mathbf{u}, \mathbf{v})$ represents the two-dimensional velocity field of the fluid (plasma) through the parathyroid gland. As a consequence of our assumptions of steady flow and mass conservation of plasma, the product of the plasma velocity u_i and the cross-sectional area A_i at the Left inflow, $u_i A_i$, must be equal to the product of the plasma velocity and the cross-sectional area $u_m A_m$ at any region in the gland (see our computational model diagram in Figure 4.2). Thus, in the broader sections of the gland, the flow velocity is $u_m = u_i A_i / A_m$, implying a smaller advection term. This is consistent with the known physiology of capillary and interstitial transport.

(c) In the organ level model simulations: The PTH secreting cells are arranged in either a uniform pattern representing a healthy control or in a non uniform pathological pattern with an area with areas of increased cell density (ρ greater than unity) inserted in between areas of normal density. Typically, we expect Reynolds number to be small ($\sim O(1)$). At present, we choose the Schmidt number to be unity. In order to mimic the increased tissue density of an adenoma (in the glandular level model), we will assign a density value rho(x,y) greater than unity.

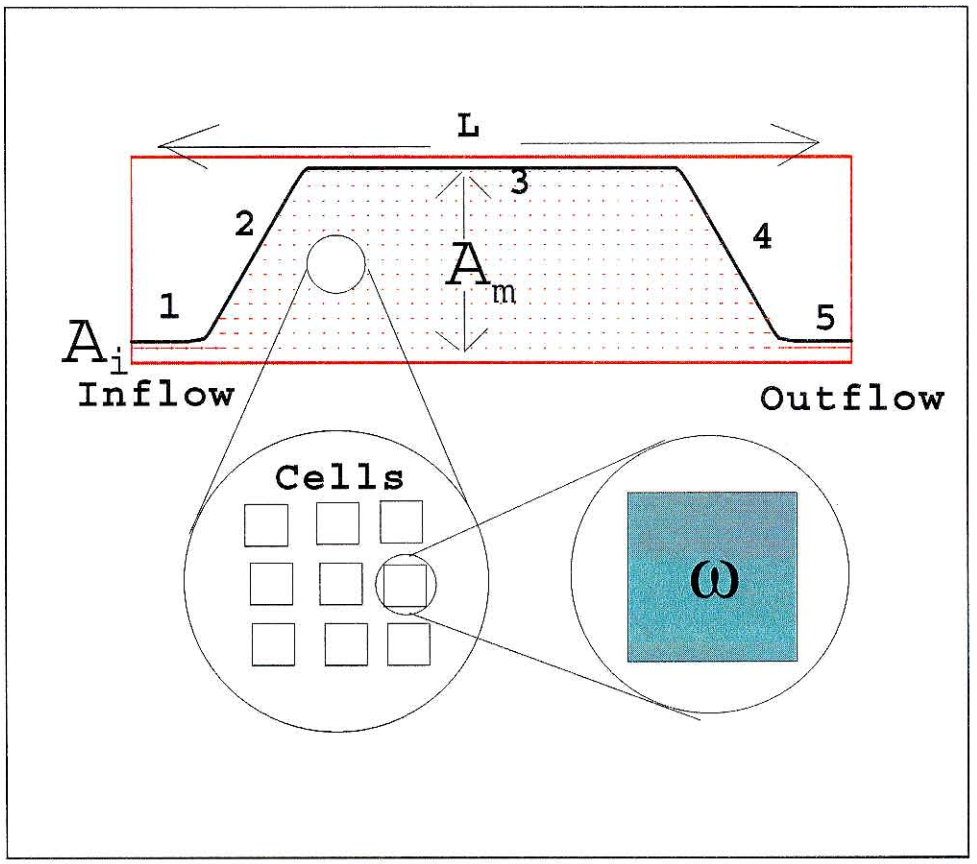

Figure 4.2: Schematic diagram of the computation model and its relationship to the simple cell model.

4.1.1 Numerical method

Glandular-level model numerical details

Our computational domain is depicted in Figure 4.2. The above coupled PDEs (4.12-4.14) are solved numerically using finite differences. We first define a Cartesian domain which is larger than the gland (e.g., the rectangle containing the gland in Figure 1). This domain is discretized with a uniform mesh of $N \times M$ with N (resp. M) points in the x (resp. y) direction. Points on this mesh are indexed by (i, j) such that $i = 1, 2, \cdots, N$ and $j = 1, 2, \cdots M$. At any point (i, j) on the mesh the advection

term is discretized using first-order upwinding as

$$\left(\frac{\partial C}{\partial x}\right)_{i,j} = \frac{C_{i+1,j} - C_{i,j}}{\Delta} \quad if u > 0 \tag{4.27}$$

$$= \frac{C_{i,j} - C_{i-1,j}}{\Delta} \quad if u < 0 \tag{4.28}$$

where Δ is the mesh spacing. The y-derivative terms are similarly discretized. The diffusion terms are discretized using second order central differences as

$$\begin{aligned} \nabla \cdot (D_c \nabla C)_{i,j} = {} & D_{c,i,j} \frac{C_{i+1,j} + C_{i-1,j} + C_{i,j+1} + C_{i,j-1} - 4C_{i,j}}{\Delta^2} + \\ & \frac{(D_{c,i+1,j} - D_{c,i-1,j})(C_{i+1,j} - C_{i-1,j})}{4\Delta^2} + \\ & \frac{(D_{c,i,j+1} - D_{c,i,j-1})(C_{i,j+1} - C_{i,j-1})}{4\Delta^2} \end{aligned} \tag{4.29}$$

The gland boundary, $\partial\Omega$, consists of the lower boundary, an inflow and outflow and piecewise linear curves (line segments numbered 1 through 5 in Figure 1) and is written as

$$\delta\Omega = \{L_q | q = 1 \cdots Q\} \tag{4.30}$$

$$L_q = \{[\bar{x}_{q,r}(t), \bar{x}_{q,r+1}(t)], r = 1 \cdots R(q)\}. \tag{4.31}$$

A "distance function" method [36] is employed to solve the PDEs in the gland domain as follows. Given the piecewise linear curves 1-5 of $\delta\Omega$, we define a *signed distance function* as follows:

$$\phi(\bar{x}_{i,j}, t) = sign \quad \min[d(\bar{x}_{i,j}, \bar{x}_{q,r}), \quad q = 1 \cdots Q, r = 1 \cdots R]$$

$$sign = +1 \quad (Outside) \quad sign = -1 \quad (Inside)$$

The region outside the gland where $sign = 1$ is referred to as the "ghost" region. Level set $\phi(\bar{x}_{i,j}, t) = 0$ defines $\delta\Omega$. Once the signed distance function has been calculated, we extrapolate the calcium and PTH concentration ($\psi \equiv (C, P)$) by advection in

pseudo-time.

$$\psi_\tau + \hat{n} \cdot \nabla\psi \quad = \quad 0, \quad \hat{n}(\bar{x}_{i,j}, t) = \frac{\nabla\phi}{|\nabla\phi|}, \tag{4.32}$$

where the advection velocity is $\hat{n}(\bar{x}_{i,j}, t)$, the normal to ϕ. Note that this advection equation is solved only where $\phi(\bar{x}_{i,j}, t) > 0$ so as to populate with the ghost mesh points with extrapolated values of P and C. Furthermore, the advection equation is solved to steady state, so that $\psi_\tau = 0$ which ensures that the zero flux boundary conditions for calcium and PTH concentrations at the gland boundary are satisfied. We would also like to ensure that there is no advection of P and C at the gland boundary. This is achieved by the same extrapolation procedure for the velocity components. The normal velocity component is then reflected in the ghost region so that there is no mass flux at the gland boundary. This step is done only once as the flow velocity is steady in our model.

The Neumann boundary conditions on the remaining boundaries are calculated using 2nd order, one-sided differencing. For the left boundary (inflow) of $\partial\Omega$, the condition for P would be

$$P_{i,j} = \frac{4}{3}P_{i+1,j} - \frac{1}{3}P_{i+2,j}. \tag{4.33}$$

The spatial derivatives are computed using centered 2nd order finite differences. We update the concentrations of calcium and PTH by explicit time-marching using a 2nd order Runge-Kutta time integration scheme [30].

The cell density is generally kept constant for normal glands while adenomas are modeled as regions of increased $\rho(\mathbf{x}, t)$. A table below gives the model parameter values used in simulations unless otherwise noted.

The model's convergence properties were evaluated by testing a known PTH calcium

Parameter	Value
α	8.00
V	1.0
κ	0.10
λ	1.00
I_0	0.40
C_0	0.95
C_{cell}	1.00
ρ	1.00

Table 4.1: A list of the gland model parameters and their values.

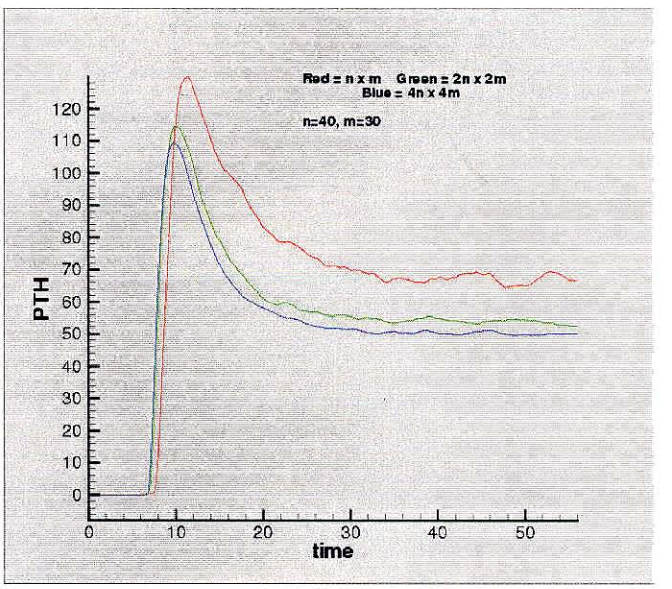

Figure 4.3: These curves represent the same "test" protocol at increasing resolution of the mesh as discussed in the text.

infusion algorithm at progressively finer mesh resolution n x m, 2n x 2m, 4n x 4m, where n=30 and m=20. The Figure 4.3 graphically displays near quadratic convergence which is expected from the 2nd order finite difference scheme.

Chapter 5 Glandular-level Simulations

In this chapter we will use the gland model to simulate published clinical studies and then compare the model results with the clinical data. In section one, we follow the protocols of in vivo infusion studies on normal and adenomatous glands. In section two, we use actual calcium data from patients (given to us by our clinical collaborators at UCLA), as the left boundary Dirichlet condition in our gland model and then compare the model output with the actual patient PTH data. In the final section we use the model to examine an interesting aspect of calcium-PTH physiology that has to date not been explained.

5.1 Citrate and calcium infusion studies

5.1.1 Citrate infusion experiment

We begin the examination of the glandular level model by following the infusion protocols published by Schmitt et al. [38]. In the citrate (PTH stimulation) study protocol, the subject's serum calcium and PTH are monitored every 2 minutes. At a designated time (75th minute), a sodium citrate infusion is introduced to lower the subject's serum calcium from a baseline (e.g., 1.20 mmol) to a designated target concentration (e.g., 1.00 mmol) at a rate of 0.01mmol/min for 20 minutes (see Figure 5.1). The new calcium concentration is then maintained for the remainder of the study. We follow this protocol computationally by prescribing a calcium concentration of 1.20 on the left boundary for the first 75 time units and then lowering the calcium to 1.00 as in the clinical study. In addition, to mimic the calcium fluctuations, we add a random fluctuation about the mean (see graph in Figure 5.3).[1].

In the actual clinical study, a vigorous rise in PTH secretion is seen within 5 minutes

[1] At minute 75 we lower the concentration linearly to reach a target of 1.00 units by minute 95 and maintain this concentration for the remainder of the simulation; see Figure 5.2

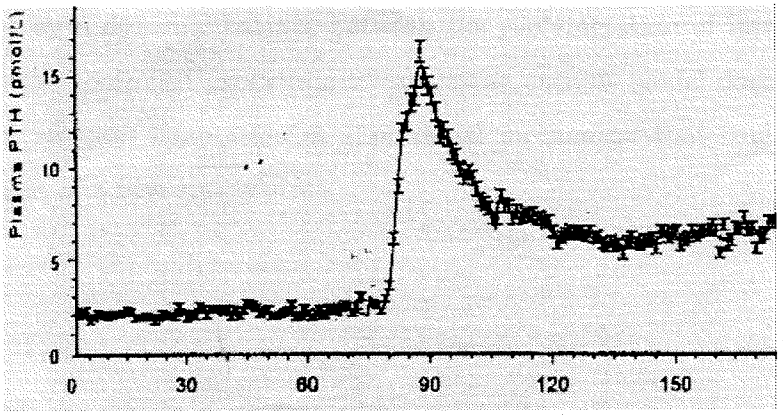

Figure 5.1: Calcium lowering infusion test and the PTH response in time.

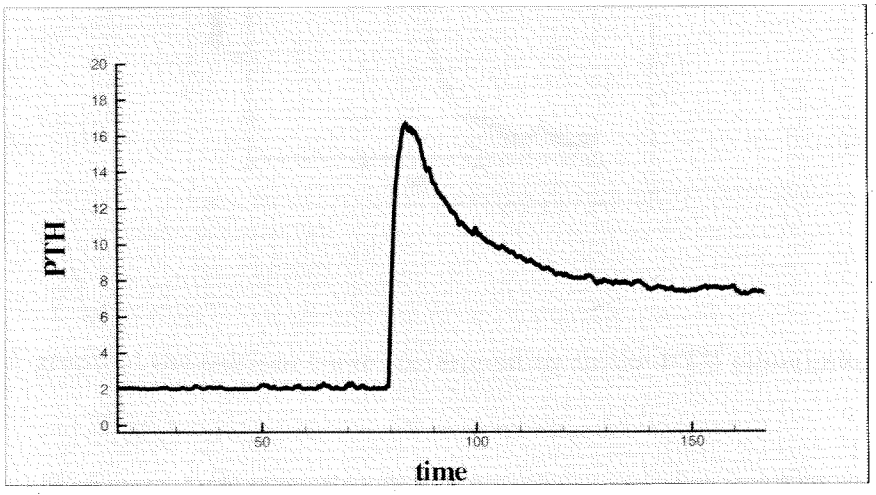

Figure 5.2: A simulation of the experimental calcium lowering protocol with the model.

of initiating a calcium lowering protocol. This is followed by a slower fall to a new steady state for the remainder of the experiment [38]. An important feature in the PTH response is that the peak concentration is reached by minute 90 and then begins to descend despite the fact that the calcium concentration continues to drop until minute 95. The computational analogue seems to capture this quality (Figure 5.2). Based on our model, we forward the following analysis. Subsequent to the initial PTH release, the cell stores begin to deplete their PTH stores and cannot maintain the maximum secretory capacity. Consequently, the PTH concentration begins to fall even though the calcium concentration continues to drop. The literature seems to support this as is shown in Schwarz et al. [39]. The fall to the new steady state

is governed by a dynamic balance between the evolving state of intracellular PTH stores and the continued exocytotic release. The current model does not explicitly account for receptor adaptation as a potential mechanism that contributes to the establishment of a new steady state.

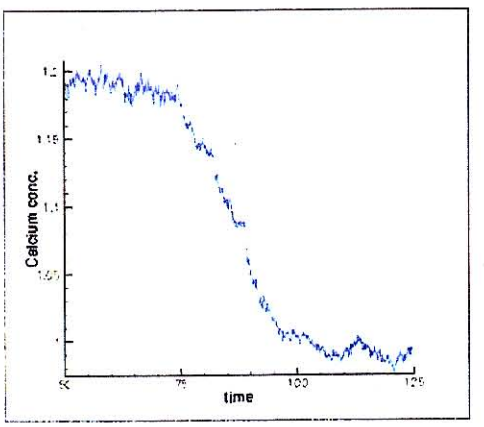

Figure 5.3: A graph of the calcium curve corresponding to the PTH stimulation protocol.

5.1.2 Calcium Infusion Studies

In a companion experiment, the protocol is identical to the above only that at minute 75, a calcium infusion is initiated instead of the citrate. The goal in this case is raising the calcium concentration by 0.2 mmol over a 20 minute interval. The experiment shows the rapid fall of PTH from a baseline of approximately 4 pmol. to 1 pmol. (Figure 5.4). The computational model follows the protocol and is able to produce results that qualitatively agree with the clinical study (Figure 5.5).

As a further evaluation of the model's ability to capture regulatory physiology, we perform a simulated calcium infusion study on our "healthy" model gland and in a model gland where we created an adenoma. The adenoma is simulated by assigning a value of 0.8 to the parameter ρ, our tissue density factor, in a specified region of the gland. The calcium infusion simulation in this case is initiated after a PTH stimulation. This is done so that the suppression of the PTH occurs from a higher

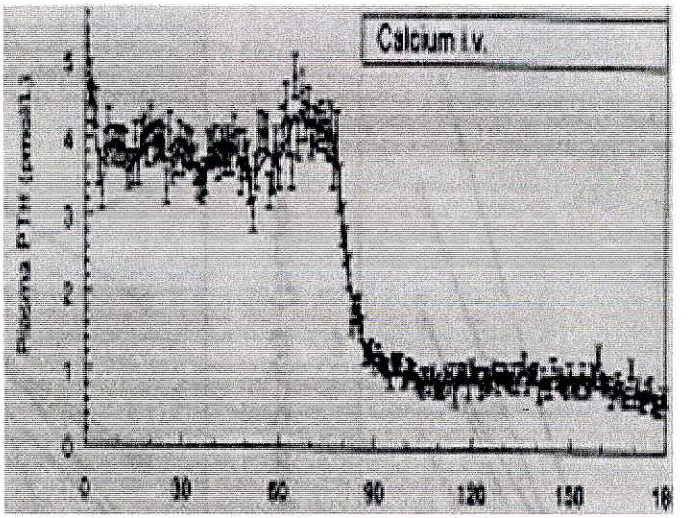

Figure 5.4: A healthy patients's PTH is inhibited by the infusion of calcium.

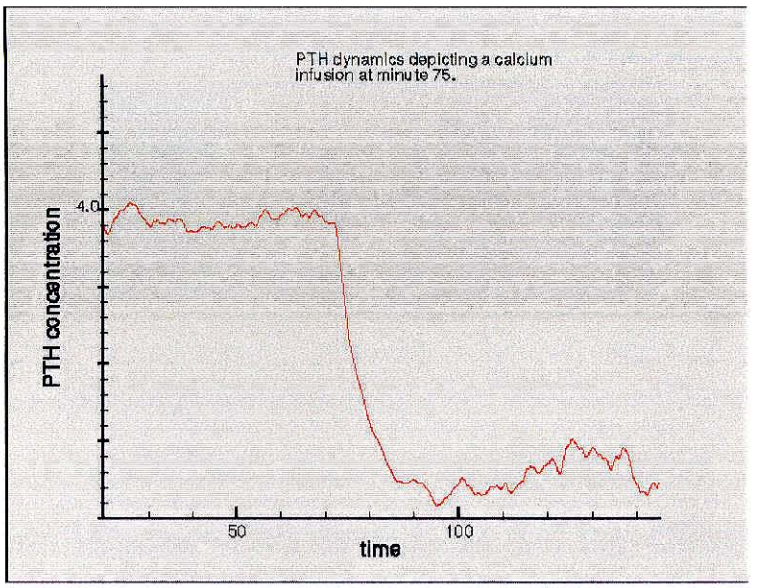

Figure 5.5: A simulation of the calcium infusion test

base concentration. Figure 5.6 depicts the calcium flow through the healthy gland and Figure 5.7 represents the flow at the same point in time in the simulation with the adenoma. Note the "bending" of the calcium concentration level curves as they pass through the denser adenomatous tissue (Figure 5.7). We now compare our results with those reported in the literature. Goodman et al. as well as others have shown

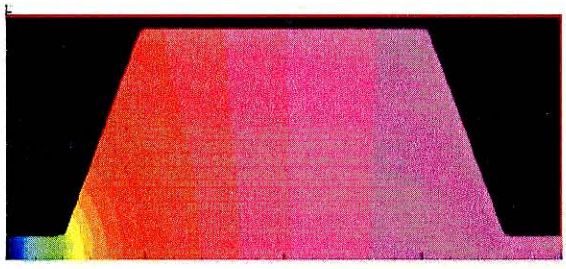

Figure 5.6: Calcium diffusion in the "healthy" gland.

that the calcium infusion tests on subjects with adenoma suppress the adenoma to a value of 25-40% of baseline. This is in contrast to the healthy subjects whose PTH levels can be suppressed to 5-10% of baseline (Figure 5.8). In the model, the calcium infusion is able to suppress the adenomatous gland from the normalized baseline to 45% of the baseline value, whereas application of the same infusion suppressed the healthy gland to 10% of its baseline over the same time period (see Figure 5.9).

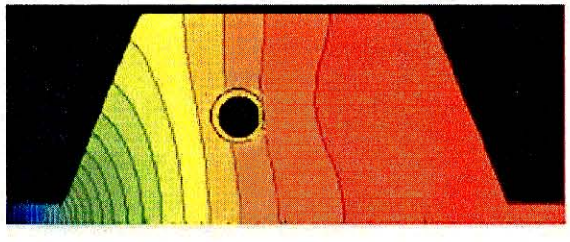

Figure 5.7: A parathyroid adenoma in the gland affecting the calcium diffusion.

5.2 Simulations with data from UCLA Center for Clinical Research

In this section, we test the model using data obtained from the UCLA Center for Clinical Research (CRC). Over the past decade, there has been an active program of research at the CRC, focusing on the macro-physiological response of the parathyroid gland to infused calcium stimulations. One of the achievements of this work has been the application of the calcium infusion technique to diagnose and distinguish pathologies of the gland: in particular familial hypocalciuric hypocalcemia (FHH),

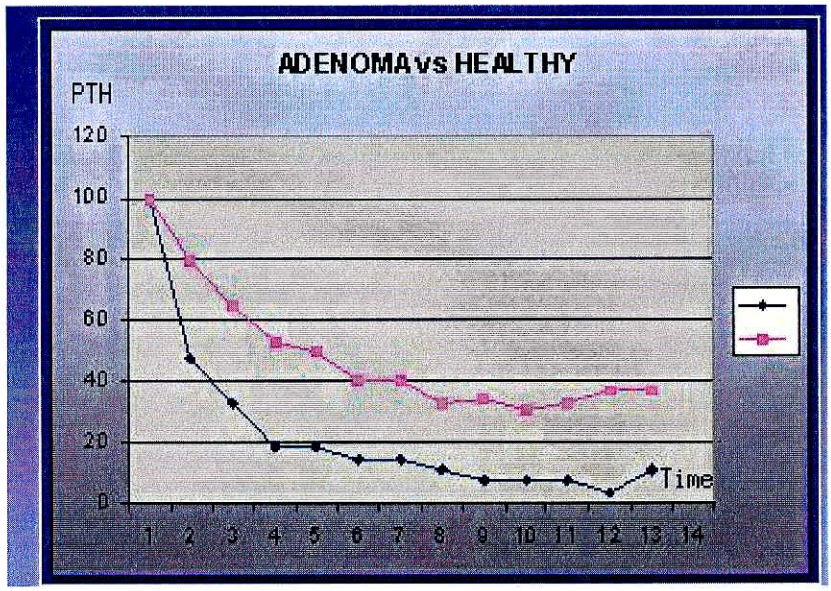

Figure 5.8: A comparison of calcium infusion tests from two patients at the UCLA Center for Clinical Research. One has an adenoma and the other is healthy. These curves have been normalized to 100% of baseline. The absolute levels commonly seen with adenoma (upper curve) can be many fold higher than normal levels.

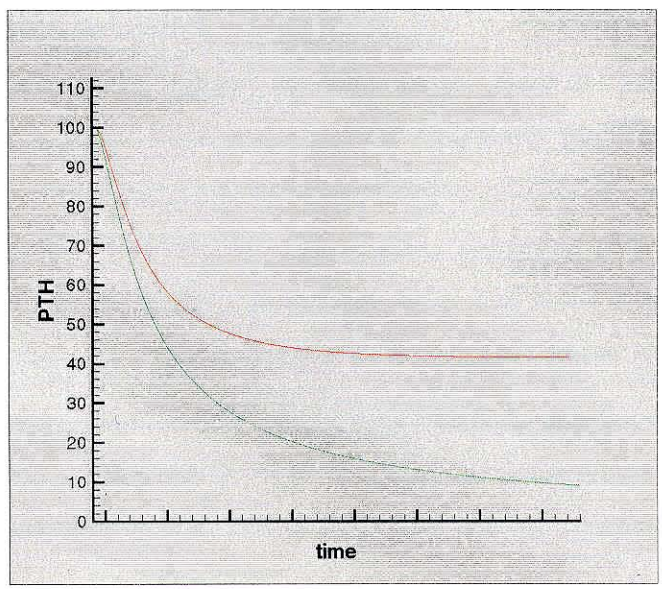

Figure 5.9: The computational analogue of the previous figure.

hyperplasia, and adenoma. The clinical distinction is critical, in that in adenoma the treatment will be surgical as opposed to FHH and adenoma where the treatment is usually pharmaceutical. We were privileged to receive several sets of data from the CRC's calcium infusion studies of both healthy controls and subjects with disease. The data sets are lists of the subject's time correlated PTH and calcium concentration obtained every two minutes. The protocol in all these studies was to slowly increase the calcium concentration in the serum by increasing the calcium infusion rate until either the PTH secretion was sufficiently suppressed or the calcium level was approaching a clinically unsafe value. In our simulations we used the patient serum calcium data as the input value of our left boundary in the gland model. The value of the calcium between the two-minute data points was obtained by linear interpolation.

Dirichlet boundary conditions are imposed on the inflow,

$$C(x = 0, y, t) = \widehat{C}(t). \tag{5.1}$$

In Figure 5.10 we compare the model PTH output to that of the healthy patient. The model seems to produce reasonable qualitative agreement with the patient PTH output. The parameter values used here are the same as those given in the model derivation section with the exception of the C_{cell} level. In order to establish a meaningful calcium threshold C_{cell} for an individual patient, we used the mean of the individual patient's calcium data as a guide. Assuming that the actual inhibitory threshold is somewhat higher, we assign a value that is 0.2 units above the mean. In this way we allow the calcium infusion to rise up and inhibit the gland.

We also tested the model on a patient with FHH. As mentioned previously, patients with FHH have a defect of the Calcium sensing receptor (Casr) which manifests clinically as higher than normal serum PTH and calcium concentrations. Surprisingly, calcium infusion suppresses FHH patient's PTH to the same degree as in healthy patients. We insert the pathology in our model by raising the cell threshold C_{cell}. Conceptually, this is consistent with reports that the defect in FHH resides in in-activating

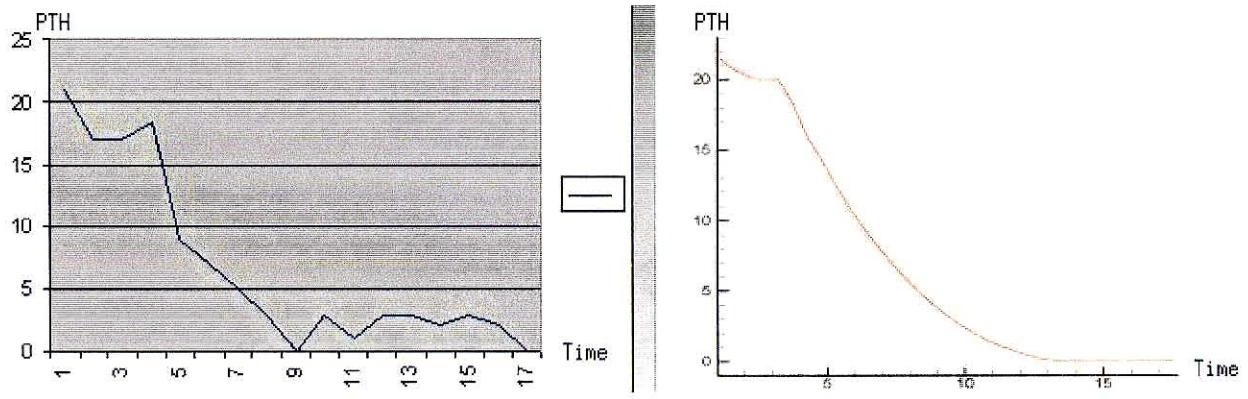

Figure 5.10: The left graph depicts a healthy subject's PTH response to a calcium infusion protocol (at UCLA Center for Clinical Research). The graph on the right is the model's output using the patients calcium as an input on the left boundary.

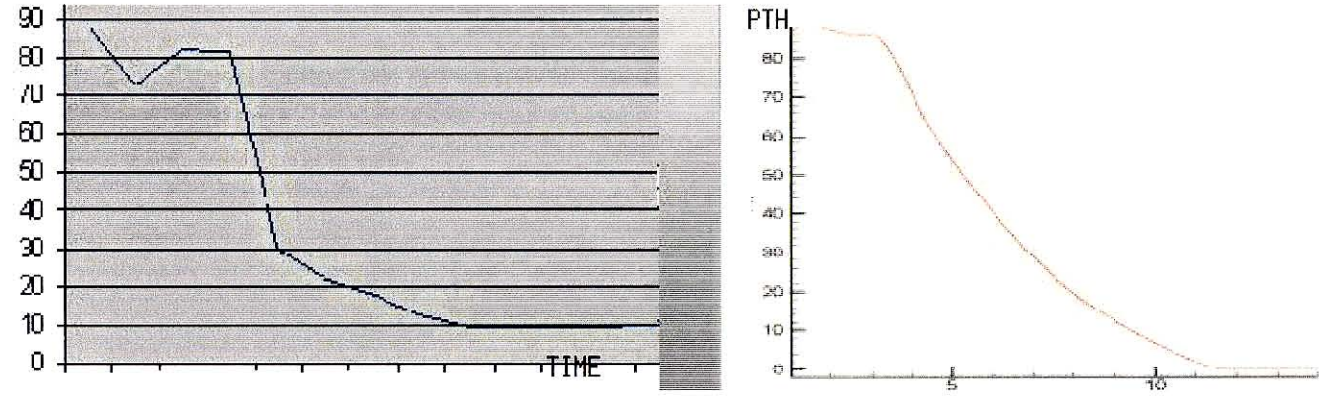

Figure 5.11: Here we compare our model output (right graph) to a patient with Familial Hypocalciuric Hypocalcemia (FHH).

mutation's of the Casr [25]; thus rendering it less sensitive to normal calcium concentrations. Once the proper intracellular signal is generated, the cellular mechanisms of inhibiting exocytosis appear to be intact. Furthermore, there are no histological changes that would affect the cell geometric arrangement, as there is in adenoma and hyperplasia. Figure 5.11 shows the results of our model and experiment respectively.

5.2.1 The asymmetry of the calcium-PTH curve

A long standing discussion in the PTH literature centered around the claim that the circulating value of PTH resulting from an infusion protocol that first lowers calcium and then returns to the baseline calcium was not equivalent with the PTH value

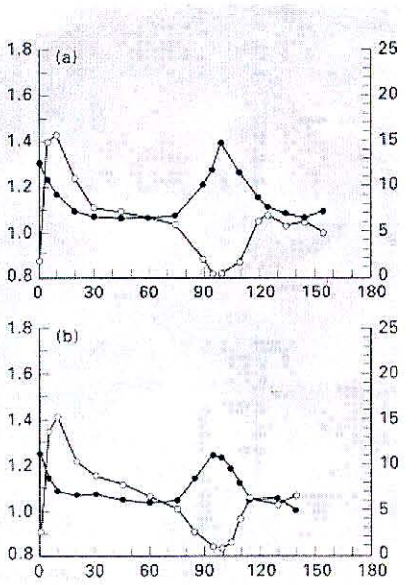

Figure 5.12: These figures are taken from Schwarz et al. The x-axis is time, calcium and PTH concentrations depicted on the left and right Y-axis respectively. The darkened circles represent calcium and the open circles PTH. Note that after the initial transient the PTH decay time is slower than the rise time.

obtained by first raising calcium and then lowering it. This behavior was partially resolved in 1998, when Scwarz et al. [39] showed that once the large initial transient

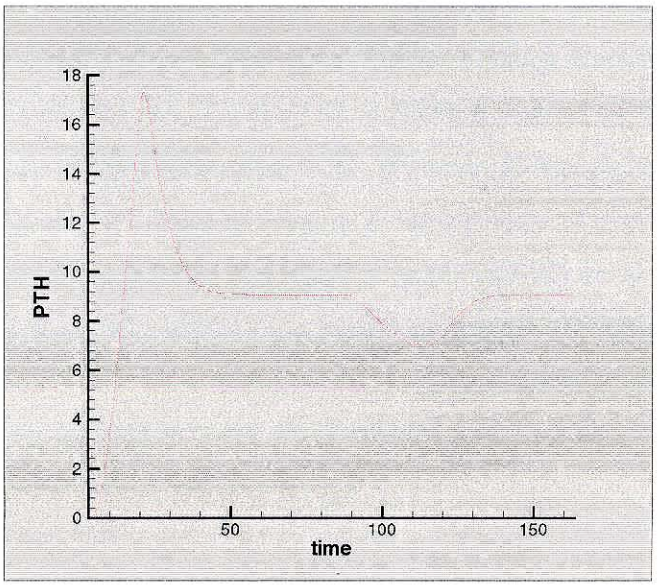

Figure 5.13: The decrease in diffusivity of the calcium in the presence of high PTH is evidenced by the asymmetry in the decay and rise time of PTH.

PTH response had occurred, all subsequent paths taken were nearly symmetric. The conclusions drawn were that the apparent "hysteresis" was largely the result of the initial release intracellular stored vesicles. A subtle point, however, remained without resolution. Investigators have noted that in infusion studies, the time it took to inhibit PTH secretion from a baseline PTH was longer than the time it took to return to the baseline. This phenomenon can be appreciated by examining the simultaneous PTH and calcium plots in Scwarz et al. (Figure 5.12). The model we have proposed would certainly predict this behavior, which simply follows from the PTH dependent diffusivity.

In Figure 5.13 we show how the glandular-level model captures this point. The protocol we use follows from the paper by Scwartz et al.

- Step one: we first lower the calcium which induces a higher PTH state.
- Step two: we then raise calcium to the higher state and the PTH level falls accordingly.
- Step three: we re-lower the calcium back to the level just prior to step two and the PTH level returns to the higher state.

As can be seen by inspection of Figure 5.13, the rise time induced by calcium lowering is faster than the decay time induced by calcium raising. Careful clinical experiments could easily clarify this point further. Experimental support for this explanation is also derived from the studies of Setoguti et al. [?] where it was shown that the production of vesicular stores of PTH did not change in the presence of hypercalcemia. Therefore, this disqualifies the argument that after a hypercalcemic event there were more new stores of PTH ready for release than after a hypocalcemic event.

Chapter 6 Extensions of the Cell Level and Glandular Level Modeling

In the first section of this chapter a refined cell-level model is presented. In the second section the gland-level model is used to demonstrate preliminary results concerning the effects of feedback, as well as testing the model with the minute to minute calcium-PTH data obtained from our clinical collaborators at the UCLA School of Medicine.

6.1 A refined cellular model

There are additional cellular level features in the Parathyroid physiology that could influence the physiological response. It is expected that the physical presence of the cell body in the interstitial space imposes further restriction on calcium's diffusivity. Furthermore, the "convoluted" cell membrane folds, in which the specialized calcium sensing receptors reside, posses apical lateral secretory polarity [49]. These cell structural features along with the secreted macromolecules collectively influence the diffusion paths of the regulating calcium molecule. The inclusion of these features is desirable and may lead to insights not possible to intuit apriori. In this section we take initial steps toward a cell model that includes a cell membrane as a separate functioning entity. The cell body will impose geometric constraints on interstitial diffusion. The model equations are presented below. We skip over the derivation, which for the most part is a repetition of the simpler cell model in chapter two. The assumptions are briefly discussed and the numerical method used is outlined. Following that we show results that parallel the results of the simple cell model presented earlier.

6.1.1 The model

Our domain Ω consisting of an interstitium containing a single cell ω and its associated cell membrane μ is shown in Figure 6.1. Our model equations in dimensionless variables are again

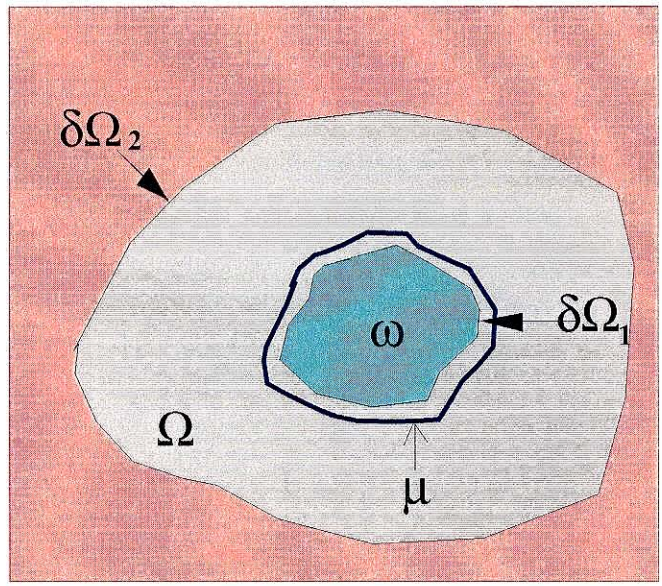

Figure 6.1: A schematic diagram of a cell ω and its surrounding membrane μ inside an interstitial space Ω.

$$\begin{aligned}
\frac{\partial C}{\partial t} &= \nabla \cdot (\exp^{-\lambda P} \ \nabla C), && \mathrm{x} \in \Omega, t > 0, \\
\frac{\partial P}{\partial t} &= \nabla \cdot (D_p \ \nabla P) + \chi(x) S(C, I), && \mathrm{x} \in \Omega, t > 0, \\
\frac{\partial I}{\partial t} &= \kappa V - S(C, I), && \mathrm{x} \in \mu, t > 0,
\end{aligned} \tag{6.1}$$

where

$$S(C, I) = \alpha\{C_{cell} - C(\mathbf{x}, t)\} I(x, t) H(C_{cell} - C), \tag{6.2}$$

and where

$$\chi(\mathbf{x}) = \begin{cases} 1 \ if \ \mathbf{x} \in \mu \\ 0 \ if \ \mathbf{x} \notin \mu. \end{cases} \tag{6.3}$$

The Heaviside function H is defined as before (see equation 2.6). It is important to note that in this model, source $S(C, I)$ is now confined to the cell membrane region μ.

Our dimensionless boundary and initial conditions are

$$\frac{\partial C}{\partial n} \equiv \nabla C.\hat{\mathbf{n}} = 0 \quad on \quad \partial\Omega, \tag{6.4}$$

$$\frac{\partial P}{\partial n} \equiv \nabla P.\hat{\mathbf{n}} = 0 \quad on \quad \partial\Omega, \tag{6.5}$$

$$\tag{6.6}$$

and

$$P(\mathbf{x}, t = 0) = 0, \tag{6.7}$$

$$I(\mathbf{x}, t = 0) = I_0, \tag{6.8}$$

$$C(\mathbf{x}, t = 0) = C_0, \tag{6.9}$$

where $\partial\Omega = \delta\Omega_1 \cup \delta\Omega_2$.

Assumptions and Jusifications

(a) The cell membrane μ replaces the function of the ω in the simpler cell model. The cell body, now represented by ω, imposes further restrictions on the diffusion paths in the interstitial domain Ω. As in the simple cell model level, we assume that the cell membrane receptor and exocytosis sites are the same. The general model depicts a cell membrane completely surrounding the cell body.

(b) In our computational model, however, we make use of an additional feature. We will choose the cell membrane to have apical lateral polarity (see Figure 6.2). The inclusion of this feature represents our current view of the PTH cell physiology. Further discussion and references are cited in the supplementary section.

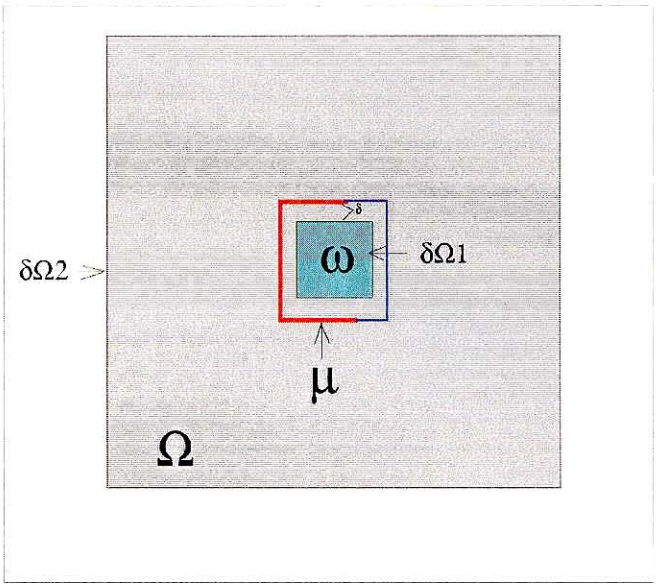

Figure 6.2: The cell level system of differential equations are numerically solved on the domain Ω and the boundary conditions hold on $\partial\Omega=\delta_1 \cup \delta_2$. The cell body is represented by ω, while the cell membrane is μ. Note that in the computational model the cell membrane μ secretory activity is restricted to the apical lateral region of our cell which is depicted in red. The blue segment of the membrane is inactive.

Cell-level model numerical details

Equations 6.15-17 are solved using the same method as in the simple cell model. Our domain Ω is discretized with a uniform mesh of $N \times M$ with N (resp. M) points in the x (resp. y) direction. Points on this mesh are indexed by (i, j) such that $i = 1, 2, \cdots, N$ and $j = 1, 2, \cdots M$.

As before, diffusion terms are discretized using 2nd order central differences as we update the concentrations of calcium and PTH by explicit time-marching using a 2nd order Runge-Kutta time integration scheme. However, certain differences in the numerics are outlined here.

In this model, we distinguish between an "outer" cell surface which is called the "cell membrane" and an "inner" cell surface which is the "cell body." The cell membrane is where exocytosis of the hormone takes place whereas the inner surface of the cell is considered impermeable. The cell membrane and cell body are separated by a uniform distance δ. The situation is depicted schematically in Figure 6.2. It is desirable to ensure that $\delta/L << 1$ to be physically relevant

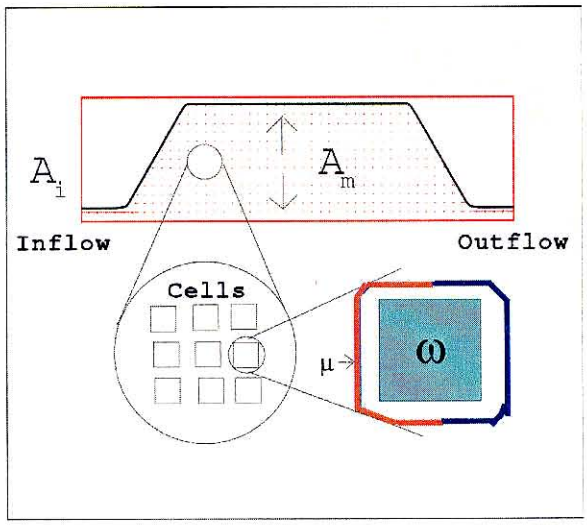

Figure 6.3: Schematic diagram showing the relationship of the refined computational cell model to the gland model.

where L is the scale of the cell size. The cell membrane, defined by μ, consists of piecewise linear curves:

$$\delta\Omega = \{L_q | q = 1 \cdots Q\} \tag{6.10}$$

$$L_q = \{[\bar{x}_{q,r}(t), \bar{x}_{q,r+1}(t)], r = 1 \cdots R(q) - 1\}. \tag{6.11}$$

Each curve L_q, has $R(q)$ points. These points represent the nodes at which calcium receptors reside and at which exocytosis occurs. A level-set method is employed to solve the PDEs in the domain as follows. Given μ, we define a *signed distance function* as follows.

$$\begin{aligned} \phi(\bar{x}_{i,j}, t) &= sign \ \min[d(\bar{x}_{i,j}, L_q), \ q = 1 \cdots Q] \\ sign &= +1 \ (Outside \ membrane) \quad sign = -1 \ (Inside \ membrane) \end{aligned}$$

This distance function is modified as: $\phi = \phi - \delta$ so that the level-set $\phi(\bar{x}_{i,j}, t) = 0$ now defines the cell body surface whereas $\phi(\bar{x}_{i,j}, t) = -\delta$ defines the cell membrane. The region inside the cell body surface where $sign = 1$ is referred to as the "ghost" region. The cell membrane is now part of the domain where the governing equations are solved. The no-flux boundary conditions for C and P

at the cell body surface are computed as in the glandular-level model by extrapolating the calcium and PTH concentration ($\psi \equiv (C, P)$) into the ghost region by advection in pseudo-time.

Recall that the governing PDEs are solved on a regular mesh, each point of which is indexed by (i, j). We need to evaluate the source term $\mathcal{S}(x_i, y_j)$ in the equation for PTH on each point (i, j) of the mesh. We first compute $\mathcal{S}$ on each node (i.e., $\mathcal{S}(x_{q,r}, y_{q,r})$) of the cell membrane by linearly interpolating calcium on the four nodes $(C(x_i, y_j), C(x_{i+1}, y_j), C(x_i, y_{j+1}), C(x_{i+1}, y_{j+1})$, surrounding the node point $(x_{q,r}, y_{q,r})$. After $\mathcal{S}(q, r, y_{q,r})$ is computed at each node, we linearly interpolate it on to the four surrounding mesh points. The equation for I is solved at each node $(x_{q,r}, y_{q,r})$ on the cell membrane.

6.1.2 Cell-level experiments

Here we repeat some of the cell experiments examined earlier with the simpler model. The simulations, though not identical, are analogous in concept. In particular, the PTH inhibition in this case is a result of letting an initially highly concentrated subdomain of calcium diffuse into the rest of the domain and inhibit exocytosis. Our interest will be to examine the contribution of cell geometry imposed on the domain in addition to the nonlinear diffusivity of calcium.

Isolated single cell PTH secretion vs PTH secretion in a group of cells

We again compare the PTH secretory response of a single isolated cell to that of a group of four cells that are spaced closely together. In each simulation the initial calcium concentration will zero everywhere except in a small subdomain. This is intended to mimic the placement of a depot of calcium placed into a cell culture chamber. The simulation is run until the PTH output has come to a steady state. Figure 6.4 shows the early stages of calcium diffusion.

In Figure 6.6 the single cell PTH response arrives at its steady state of 5.6 in approximately 8000 timesteps. We now perform the simulation with a group of four cells, arranged in a huddle, so that the secretory portions are facing toward the center of the group (see Figure 6.5).

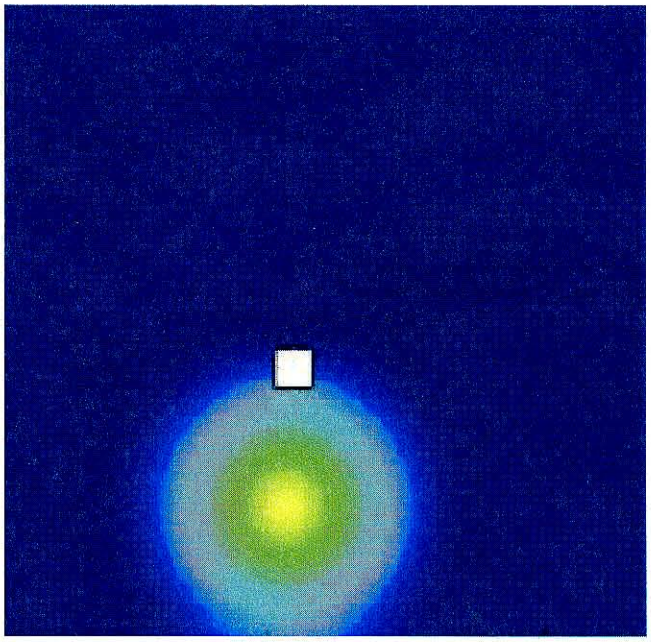

Figure 6.4: Here we show the simulation domain. An initial depot of calcium (green circle) will eventually diffuse over the cell (white square) and inhibit PTH secretion.

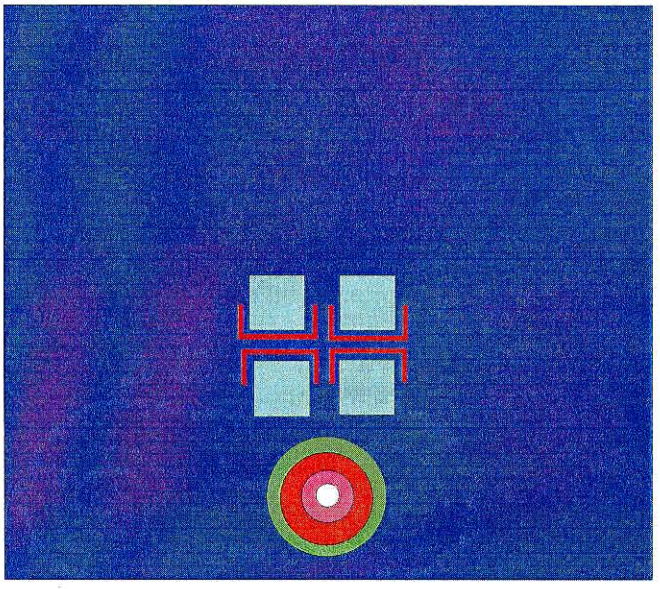

Figure 6.5: A schematic drawing of four cells with apical lateral secretory membrane (red) arranged in a "huddle." A depot of calcium is seen diffusing below the cells.

In this experiment a " depot" of calcium is placed in the domain so that the mean distance from the group of four cells is the same as the distance from the depot to the single cell. The experiment with the group of four cells shows that

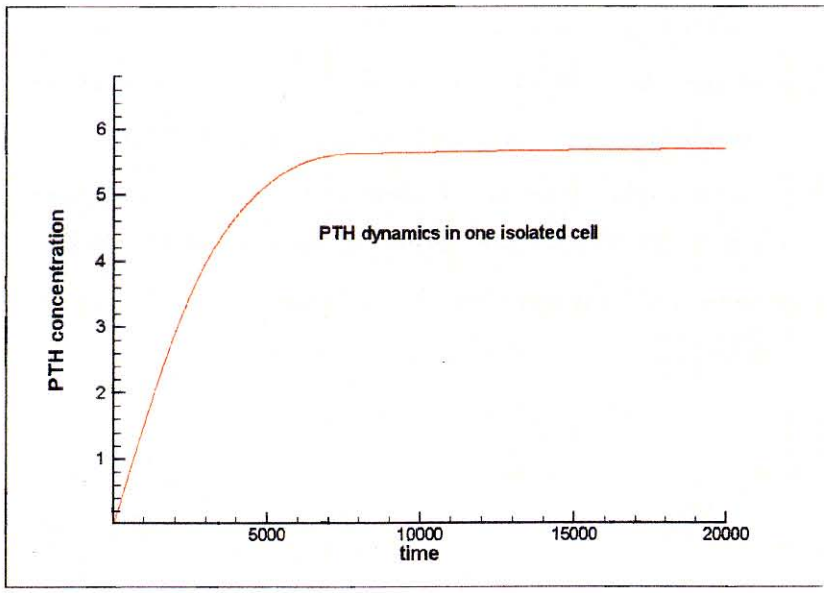

Figure 6.6: The steady state PTH concentration reached by the isolated single cell is 5.6.

the steady state of 33 is achieved by approximately 10,000 timesteps. The PTH secretory response for the average cell in the group is 8.25 which is clearly greater than the single-cell output of 5.6.

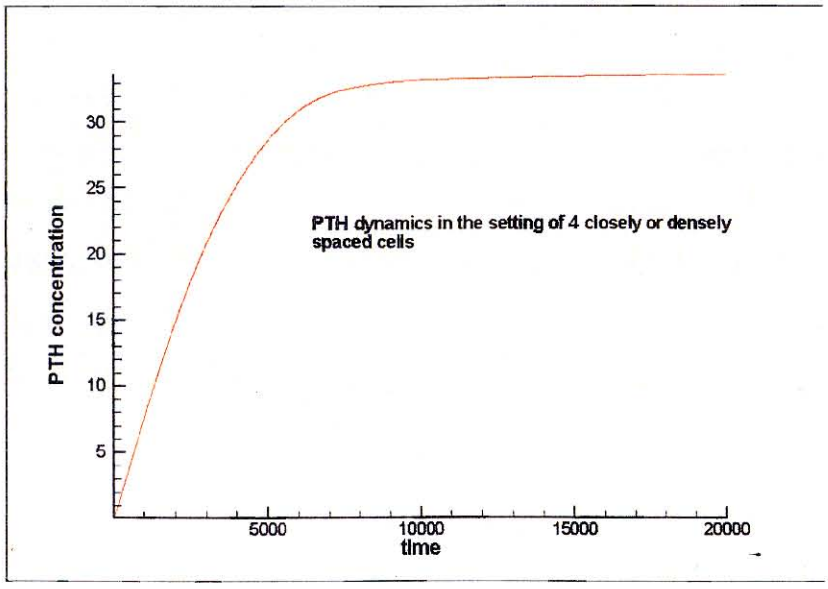

Figure 6.7: This curve shows the PTH response of a group of four closely spaced cell in our cell-level domain. The steady state reached is 33.

If the group response were a linear sum of individual single cells, the total for the group would simply be four times the value of a single cell, which in this case is

22.4. The combined effects of geometric spacing and PTH concentration result in a nonlinear increase of PTH secretion for the cells residing in a group. In our formulation the contribution of the higher PTH concentration and the spacing between cells are intimately tied. In an actual experiment these effects would be difficult to decompose. However, computationally it is possible to examine the contribution of each. We address this aspect as follows. Because we have constructed discrete receptors on the cells, we are able to shut off the receptor activity individually. Therefore, we repeat the simulation of the group of four cells as follows:

- We turn off all the receptors from three cells and leave only one active cell that has the same receptor number as the isolated cell.
- We choose to keep the receptors on the cell that is closest in proximity to the calcium depot.
- We conduct one experiment with the diffusion coefficient D_c as described in the model and a second experiment with the free diffusion coefficient for calcium D_{c^*}=1.

As can be seen from Figure 6.8, the single cell in a group produces a steady state PTH response of 9.6 compared to 5.6 of the isolated cell. We repeat the same experiment once again, this time using D_{c^*}, the free calcium diffusion coefficient, instead of D_c. The resulting steady state PTH of 9.0 demonstrates the significant contribution of cells as obstacles to calcium diffusion independent of the effect of PTH on calcium diffusivity (Figure 6.9).

The particular choice of geometry and the empirical choice of the diffusion coefficient will, of course, influence the contribution of each component on PTH secretion. Our model construction can certainly address this question once more precise structural, physical, and biochemical data is obtained.

An additional point should be made here. Assuming that the release of PTH depends on the transport of calcium, we should therefore expect a delay in the inhibition of PTH corresponding to the speed of diffusion. The model predicts a rise in PTH slope that is faster for the group than the single cell. This can be seen by noting that the average group PTH level (total divided by 4) at time

5,000 is approximately 7 versus 5.4 for a single cell. This observation has clear parallels in the glandular-level physiology. Our computational model does not include the possible inhibitory effects of Chromogranin A. Drees and Hamilton [12] have shown that in vitro chromogranin A degenerates and breaks down into pancreastatin, which is known to inhibit PTH secretion. These effects are reported to occur on a time scale of 30-60 minutes. Chromgranin A is a relatively large protein 50kd and, in high enough concentrations, could potentially influence calcium transport. One can argue that the in vivo probability of the molecule remaining in the interstitial area long enough to degrade into pancreastatin is not high and thus not dominant in autocrine regulation of PTH secretion. Designing experiments to clarify this issue would be valuable. The effects of geometry of the cell membrane is in reality even more complex than what we have described. The convoluted membrane is not a static structure. The membrane becomes curved when the interstitial calcium concentration is reduced from a baseline concentration [?, 48]. The precise mechanisms that govern the membrane shape are unknown. In addition, it is certainly possible that the calcium sensing receptors will change in number and perhaps in distribution as an adaptation to a new calcium concentration [22]. There is no literature regarding parathyroid cell receptor adaptation available.

6.1.3 Density effects

Just as in the simple cell model, the effects of crowding or cell density [45] is just a special case of the group versus single cell experiments. The reasoning is as before. It is anticipated that if two identical cells are spaced far enough apart from each other and equidistant from a common source of calcium, they would behave individually as isolated cells. The same cells positioned closer together will exhibit the nonlinear effects seen in the simulation of the group of four cells. We demonstrate the principle visually by comparing the PTH production of two closely space and two more distant cells in the figure below. In this simulation, we had to again remain aware of the distance between the calcium source and the receptors on the cells. The result is seen in Figure 6.10 and Figure 6.11.

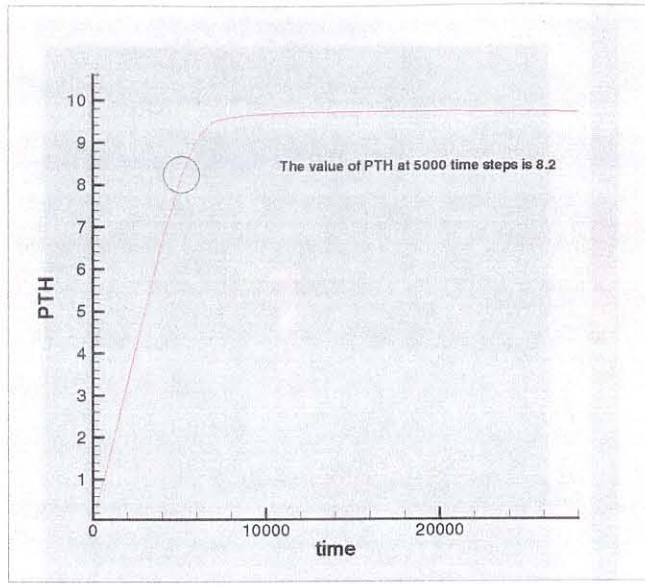

Figure 6.8: This curve shows the PTH response of a group of four closely spaced cells and only one cell possesses functioning receptors.

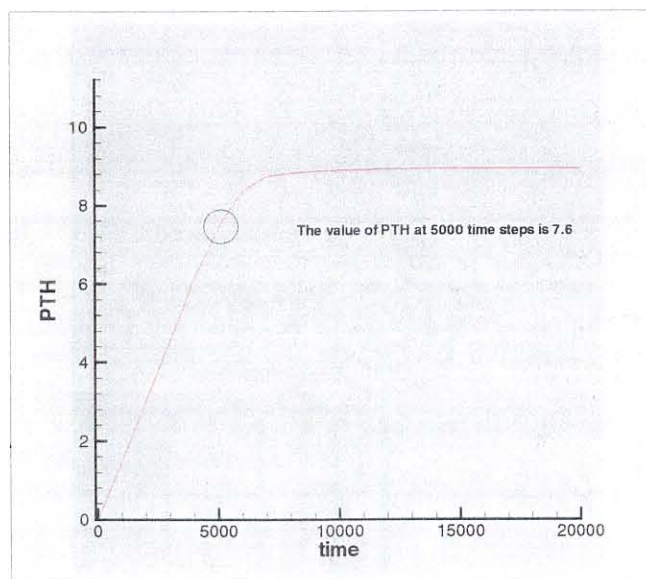

Figure 6.9: This curve shows the PTH response of a group of four closely spaced cells with the nonlinear diffusivity turned off, i.e., D= D_{c^*} and one cell only has active receptors. The steady state PTH in this case is 9.0 compared to 9.6 in the case when the nonlinear diffusivity is present.

6.1.4 Adenomas, Hyperplasia and Diffusivity

In order to illustrate how interstitial calcium diffusion might play a role in hyperplasia or adenoma, we designed a simulation of an in vitro experiment that

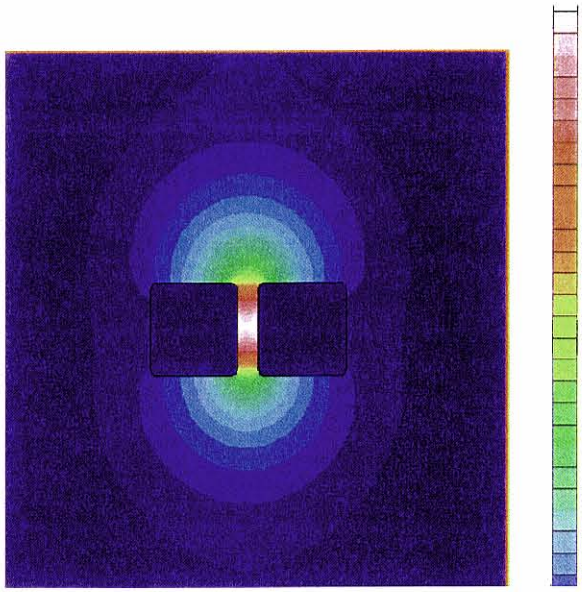

Figure 6.10: Density effects show the increased PTH secretion when the two cells are closer as seen by the higher PTH secretion (white color on the colored legend).

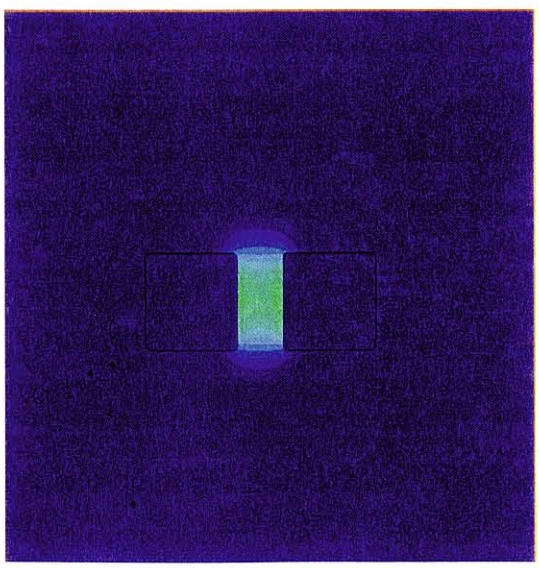

Figure 6.11: The two cells are spaced farther apart and the PTH secretion is lower.

contains a small number of adenomatous (larger and denser) cells within a cluster of normal cells. We place a small but highly concentrated depot of calcium near the adenomatous cells and let it diffuse. The smaller square cells represent healthy PTH secreting chief cells with the apical portion (secreting end) oriented toward one another. The larger, more closely spaced cells represent adenomatous

cells. In this simulation, we track the diffusion of calcium which initially is O.60 non-dimensional units (blue) everywhere except for a small patch of increased calcium concentration (3.00 (white)) just to the left of the adenomatous cells. Figure 6.12 shows the calcium diffusion early in the simulation and Figure 6.13 shows a later view. As is evident from the figures, the interstitial calcium diffusion spreads among the normal cells but sweeps around a cluster of three more densely packed adenomatous cells.

In the configuration of Figure 6.13, the low calcium concentration in the heart of the adenoma implies higher PTH secretion while the higher calcium levels in the surrounding normal cells suggest relatively suppressed PTH levels, a physiology consistent with that seen in clinical experience [54, 15]. In vitro experimental evidence of this effect is suggested in Yu et al. [54] where it was shown that adenomatous cells, while residing in a connected group, persisted in PTH secretion at given calcium concentration that was subsequently inhibitory to the same group after their dispersal into smaller groups. The argument for hyperplasia is qualitatively the same. In the glandular level (*in vivo*) there may be sufficient differences in the tissue density distribution to extract a distinguishing behavior. The results for adenoma and hyperplasia could perhaps be even more striking if we reduce the receptor number in the tumor cells and incorporate more realistic geometries. However, the qualitative principle was our first goal.

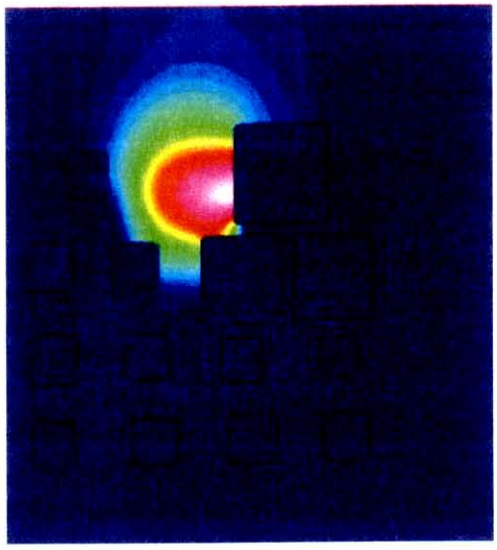

Figure 6.12: Density of adenoma effects show the resistance to calcium diffusion despite the depot of calcium placed next to the tumor (large cells). This figure is the early part of the simulation.

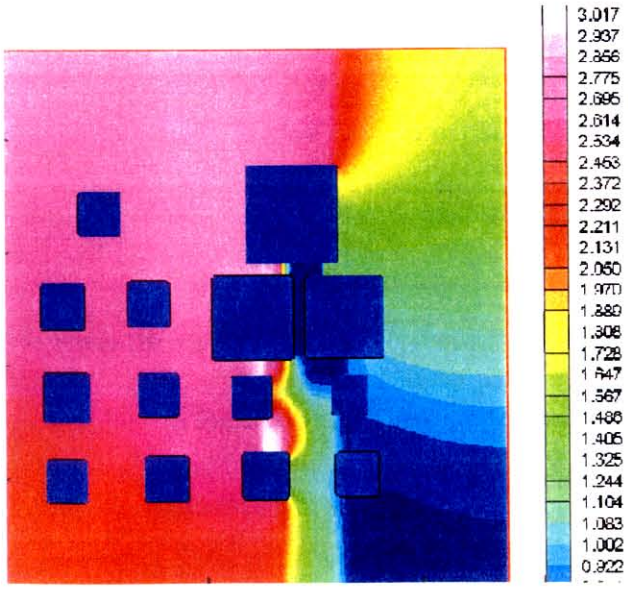

Figure 6.13: Density of adenoma effects show the resistance to calcium diffusion despite the depot of calcium placed next to the tumor (large cells).

Chapter 7 Future work

Here we very briefly describe some areas of research that we hope to pursue in the future.

7.1 Further glandular experiments

7.1.1 Pulsatility of PTH: phenomenology and conjecture

The research in Parathyroid physiology over the last decade has provided evidence that the PTH secretory pattern is characterized by intermittent pulses or episodes. The etiology of the pulses remains unknown. The ability for the Parathyroid gland to respond to calcium changes in a high gain fashion is the hallmark of healthy physiology. Blunted responses are typically seen in hyperplasia and adenoma. In accordance to our hypothesis, we conjecture that the PTH released from the gland will naturally lower or raise the systemic calcium levels and that the feedback of this calcium creates the episodic secretory pattern. In preliminary experiments using a very simple feedback condition, we have observed oscillations in PTH. We plan to expand this research and explore the contribution of gland size and the various time scales that are active in the full physiological process.

7.1.2 Minute-minute calcium data and correlated PTH secretion

Aside from the infusion studies, the UCLA group has also provided us data from studies that are investigating the correlation between minute-minute calcium and serum PTH . We have conjectured that the near sub resolution calcium levels were responsible for these PTH episodes. The difficulty remains in the poor sensitivity of the clinical measurements used. We fed several of these minute-minute data sets into the model as inflow dirichlet conditions. One such simulation is depicted in Figure 7.1 along with the corresponding actual PTH from the patient. Though

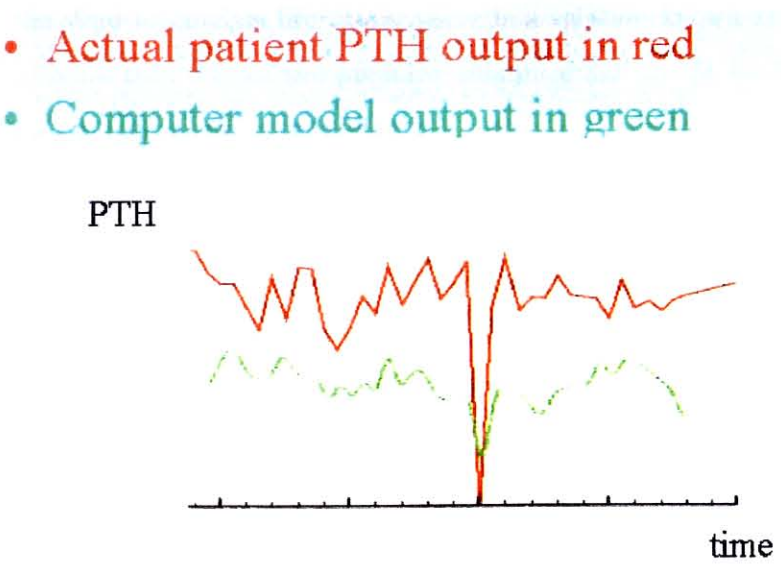

Figure 7.1: The upper curve represents the "real"patient PTH output. The bottom curve is the PTH output generated by inputing the patient's calcium data.

some of the features seen in the patient output data seem to be similar to the model output, the result is still far from satisfying. The acquisition of many more data sets will be helpful in calibrating and optimizing parameters in the model. This work is still in progress.

7.2 Biophysics and biochemistry to be investigated

7.2.1 Exocytosis and membrane curvature

It has been observed that during exocytosis, the cell membrane is described to be "convoluted"or highly curved (see Figure 9.3). The literature suggests that this may in part be due to the addition of excess bilipid membrane that has fused into the cell membrane from vesicles that store the product to be exported. The nature of intracellular transport of vesicles in the cell cytoplasm is a subject of ongoing research. If we assume that intracellular vesicles are in general exhibiting a random motion, how then can we account for the apical lateral exocytotic process (see Figure 1.5)? Suppose that a segment of cell membrane of sufficient length can be treated as a continuous structure. If we further assume that the pressure difference across the membrane is constant, then borrowing from

the fluid mechanics literature, there is a relation known as the Laplace-Young formula that relates the pressure difference ΔP to the surface tension and the radii of curvature R_1 and R_2 [2].

$$\Delta P = \sigma \left(\frac{1}{R_1} + \frac{1}{R_2} \right)$$

For a fixed pressure difference ΔP, smaller radii of curvature [1] imply a smaller surface tension. A vesicle colliding with a highly curved segment of the cell membrane would more likely fuse with the lipid bilayer and proceed with the exocytotic process. Therefore, provided there is a mechanism that initiates the change in membrane shape, the exocytotic process could in part be explained by the random motion of vesicles and the Laplace-Young formula. An interesting extension of our current model would be to incorporate the relevant intracellular physiology involved in exocytosis. This would enable us to examine the effects of cellular activity on glandular behavior in a more precise and testable way. Bridging the multiple length and time scales involved in this biology will no doubt be a daunting challenge.

7.2.2 Signal transduction

Another research objective of this work is to couple the extracellular-system level physiology to that of the intracellular signaling dynamics. As discussed in the background section, it is presumed that Ca binding to the calcium sensing receptor initiates the hydrolysis of PIP2 to inosital 1,4,5 triphospate and diacylglycerol resulting in loss of PIP2 [42]; which is active in cytoskeleton-cell membrane adhesion. Thus the IP3-Ca pathway may be closely coupled with the exocytotic process. It is also known that IP3 and calcium exhibit oscillatory activity and that while oscillations are occurring, PTH secreting cells are in the inhibited mode. The resulting calcium oscillations seen have a period of 10 seconds. As mentioned before, an ongoing challenge in this area will be to appropriately match the systems across both time and spatial scales. In a preliminary effort, we have implemented a known IP3-ca system of equations computationally, and

[1] Smaller radii of curvature in this case is the situation when the membrane assumes a shape with multiple involutions resembling fjords on a coastline.

are poised to couple these intracellular dynamics to the extracellular physiology. The crucial issue is determining the appropriate coupling.

7.3 Computation and experimental efforts

A significant test of the diffusional regulation will be to scale up the cell level model to a glandular level model without the approximations made in the current work and compare the two models. This would likely require the use of large scale computational power. The gains would be that more realistic biophysics could be examined and the lessons learned may help construct an improved reduced model for the use of clinical diagnostics.

There exists an ongoing collaboration between our group here at Caltech and the UCLA Center for Clincal Research. One of our objectives has been to design a protocol for the calcium infusion studies that would help distinguish pathologies of the parathyroid gland based on our present understanding of the physiology. The fact that our model is able to reproduce many of the clinical features seen in these infusion protocols is encouraging.

Additionally, we have already obtained permission to perform imaging studies on healthy and adenomatous parathyroid tissue by confocal microscopy. These studies will help us determine the effects of geometry and PTH concentration on the diffusion of calcium *in vitro*.

Chapter 8 Conclusions

8.1 Summary and conclusions

The effort in this thesis has been to explain and unify a set of physiological phenomena that occur both on the cellular level and on a macro-physiological level. The motivation was derived from the desire to account for two sets of "paradoxical" observations which could be condensed into two representative problems.

i. Why do single isolated cells secrete less hormonal product than single cells residing in a group?

ii. How can we explain, on the one hand, the exquisite sensitivity of in vivo PTH secretion to small changes in serum calcium (infusion studies) and, on the other hand, the claim that calcium levels and PTH secretion are not correlated in minute to minute (non infusion) clinical studies?

These questions led us to posit that the transport of the regulating molecule, calcium, was affected by both the geometric configuration of the cells in the gland and by the presence of proteins in the intercellular space. Based on this principle a mathematical model was constructed. The simulations based on our implementation of the model agree qualitatively with experiments in several categories, including the single cell versus group of cells behavior, the in vitro resistance of an adenoma, the normal in vivo response in infusion studies, as well as the pathological responses seen in familial hypocalciuria hypercalcemia (FHH). The notion that small sub-resolution calcium changes are responsible for the PTH secretory pattern is suggested by our results but falls short of actually being proven. As outlined in the discussion concerning future work, the resolution of these questions is expected to come from a combination of model refinement and the careful design of validating experiments. If we accept for the moment the idea that endocrine glands regulate interstitial transport by design, the efficiency gained by configuring cells in patterns, such as those in the parathyroid gland,

suggests a rationale for the existence of endocrine systems as organs as opposed to a dispersed system of isolated cells. The healthy gland confers robustness to the general physiology of the organism by enabling the organism to maintain a nearly constant serum calcium level in the face of countless calcium dependent processes that operate concurrently. The importance of calcium to these cellular processes rivals that of glucose and oxygen. In a sense, the diffusion mediated regulation serves an intermediate or meso-physiology between the micro-physiology of the cell and the macro-physiology of the system.

Although this work is focused on a special biological system, it raises interesting questions regarding the design of other endocrine or biological systems and potentially non-biological systems that depend on diffusion for delivery of a regulating agent and at the same time export product that influences diffusive transport. A practical application of this work may be found in the treatment of malignant tumors. Solid tumors frequently secrete large quantities of proteins that interfere with normal physiology. Quite often clinical oncologists complain that tumor size impedes chemical therapy and that "debulking" or tumor size reduction allows for increased sensitivity to intravenous cancer treatment. It is certainly possible that the insights gained from understanding the parathyroid physiology in the present work can be applied to these situations. A treatment algorithm based on a physiologically sound mathematical model would allow physicians to contemplate a new set of drug delivery strategies not easily anticipated from clinical intuition. Such a contribution would certainly open the eyes of the scientific-medical community to the virtues of mathematics as applied to the life sciences.

Chapter 9 Supplementary Material from the Endocrine Literature

9.1 Supplementary material

In this section the reader will find further biological and medical details that have contributed to the model construction. The reader will find some of the material to be redundant with the synopsis given.

9.1.1 Further reference material regarding the glandular level physiology

The clinical syndrome of excess parathyroid hormone secretion

Already from the first identifiable clinical cases of parathyroid disease, the devastating toll on skeletal mass and vital physiological processes were notable [51]. The most well known of the early clinical examples (circa. 1920) was Captain Martel of the Merchant Marines. In a textbook of endocrine disorders, the captain is shown in a photograph as a robust 6 foot 2 inch tall man of approximately 30 years of age. The companion photograph depicts the captain at age 45 having lost nearly a foot in height as a consequence of demineralization of his bone mass due to an excess in parathyroid hormone secretion. Subsequently, the parathyroid hormone (PTH) was established to be the dominant metabolic regulator of plasma calcium levels (Figure 1.1).

Plasma and extracellular calcium concentrations are essential for an impressive number of vital functions varying from cardiac contraction, nerve conduction blood coagulation and regulation of enzymatic processes. PTH is a peptide hormone that controls the level of the ionized calcium in the blood and extra-cellular fluids. PTH binds to cell surface receptors in bone, intestine and kidney and triggers responses that increase blood calcium [51]. The increase blood calcium feeds back on the parathyroid gland to decrease the secretion of PTH (Figure 1.2).

There are several other clinical entities that have more subtle parathyroid abnormalities, including osteoporosis and hypertension. The relationship of PTH secretion in these other clinical conditions is less clear and therefore emphasizes the need to understand the basic physiology of the parathyroid system in health. The time for the full PTH-calcium feedback loop process is uncertain because the feedback is a product of physiological processes on several different time scales. The renal-parathyroid loop, in health, may be on the order of tens of seconds, whereas the contribution from the intestine via vitamin D and bone mass (through osteoclastic activity) may take hours [51]. Pharmacokinetics studies that have tried to characterize the general calcium response to a controlled infusion of synthesized human PTH (Teriparatide) have been inconclusive [53].

It is presently believed that serum calcium concentrations are constant on a minute-to-minute time scale. This view frustrates the mechanistic concept that extracellular calcium changes determine short term PTH secretion. On the one hand the infusion experiments confirm the calcium's dynamic control on a time scale of minutes. In apparent contradiction, non-stimulated experiments suggest that calcium concentration (clinically measured) is constant or at best uncorrelated with the episodic PTH fluctuations. The limits of clinical ion sensitive electrodes resolve extracellular calcium down to the 10-micromolar range [19]. Unpublished data from Bill Goodman and Isidro Salusky at UCLA now suggest that there may be structure to what was thought to be noise about a steady signal. We will propose that this poorly resolved calcium fluctuation may be responsible for the observed PTH episodic pattern.

A phenomena often cited in the calcium clamp literature is "hysteresis" [10, 39]. Conlin et al. and others show that the level of PTH seen is related to the "path" history of the calcium concentration. Clinical clamp protocols that begin with lowering serum calcium then maintaining a fixed level of calcium realize a different value for PTH than if they had initially raised the calcium prior to lowering it. Scwarz et al. explain this on the basis of the availability of preformed intracellular vesicle-stored PTH as shown in [39]. We will try to unify these phenomena in our diffusion-mediated principle. Schmitt et al. published data on clamp studies of patients with secondary parathyroid hyperplasia associated with renal

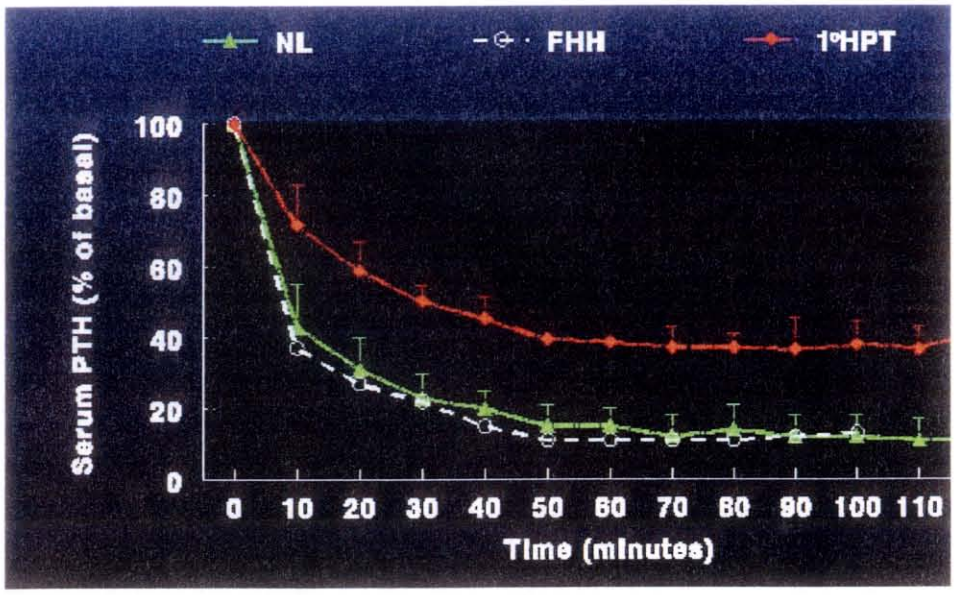

Figure 9.1: Calcium infusion tests in three cases. The red curve represents an adenoma and the green is FHH. The white curve is a healthy control.

insufficiency [?]. These patients showed a shift in their basal calcium threshold. This amounts to necessitating a higher calcium concentration to achieve the same PTH output. These patients also exhibit a blunted response to the rapid induction of hypocalcemia. Patients with primary hyperparathyroidism from both hyperplasia and adenoma both show blunted responses to calcium infusion compared with normal subjects. The genetic syndrome of Familial Hypocalciuric Hypocalcemia displays an intermediate type of behavior to the calcium infusion test [15]. While the baseline PTH secretory level and serum calcium may be high, following a calcium infusion that surpasses a threshold, the PTH secretion suppresses to the same level as do normal controls. See Figure 5.8.

9.1.2 Supplementary material regarding the cell-level physiology

The calcium sensing receptor

PTH is a relatively small peptide (approx.5000 mol.wt.)[22, 4] that controls the level of ionized calcium in the blood and extra cellular fluids. The release of PTH by means of exocytosis is presumed to be mediated by a specialized cell membrane bound calcium sensing receptor. The calcium sensing receptor (Casr)

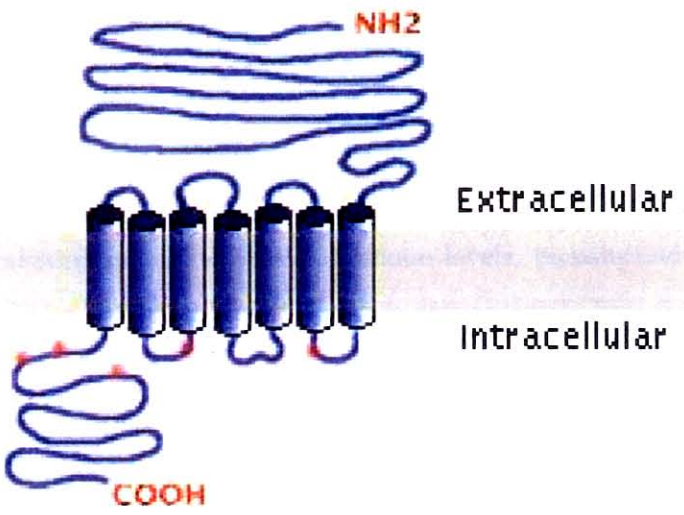

Figure 9.2: The calcium sensing receptor is believed to have a structure similar to the G-protein family of receptors.

has been cloned and shown to be a member of the G-protein coupled family of receptors [51]. The amino acid sequence suggests that it spans the membrane seven times (Figure 9.2).

A large extracellular domain resembles similar domains such as glutamate receptors, which are designed to bind small ligands such as cations [20]. The receptor has been expressed in a number of cell types where it activates phospholipase C and blocks cyclic AMP production, as it does in normal parathyroid cells [42]. Convincing evidence for the sensor came with the finding that patients with familial hypocalciuric hypercalcemia (FHH) have inactivating mutations of the calcium sensor gene [25]. Patients with FHH are reported to have blunted responses to changes in [CA]E not unlike those seen in hyperplasia. Calcium-sensing receptor number per cell has been correlated with PTH secretion. When the calcium-sensing receptor has been investigated in primary hyperparathyroidism and secondary hyperplasia, the calcium receptor number was reported as low as 30% of healthy controls [51, 4]. In a study by Ho et al [18], mice lacking the calcium sensor were shown to have all the features of severe hyperparathyroidism. Mice lacking the calcium-sensing receptor (Casr) were created to examine the receptor's role in calcium homeostasis and to eluci-

date the mechanism by which inherited human Casr gene defects cause diseases. Casr+/- mice, analogous to humans with familial hypocalciuric hypercalcemia (FHH), had benign and modest elevations of serum calcium, magnesium and parathyroid hormone levels as well as hypocalciuria. In contrast, Casr-/- mice, like humans with neonatal severe hyperparathyroidism, had markedly elevated serum calcium and parathyroid hormone levels, parathyroid hyperplasia, bone abnormalities, retarded growth and premature death. The findings suggest that Casr mutations cause these human disorders by reducing the number of functional receptor molecules on the cell surface. In a study by Kifor et al. [22], the calcium sensor was found to be localized in caveolin rich domains. Caveolin has been associated with exocytotic locations on the cell membranes surfaces [1]. The potential consequences of the receptor distribution localizing to regions of secretory activity add weight to our hypothesis, which depends on geometric considerations as well as biochemical processes. (See hypothesis section.) Recently synthetic calcimmimetic compounds have been developed that act at the level of the calcium sensor and enhance the sensitivity of the sensor to extracellular calcium concentration [25], thus leading to greater inhibition of PTH release for a given calcium level. Clinical trials using some of these agents have been conducted for patients with adenomas and with success. Parathyroid hyperplasia is known to occur as a result of renal insufficiency. A further study suggests that the use of calcimimetic compounds prevents the development of hyperplasia in nephrectomized animal studies. There are other mechanisms sited in the literature that induce PTH secretion by non receptor mediated paths [?, 6].

Cell signaling

The binding of calcium to the sensor inhibits PTH secretion into the extracellular space from its stored intracellular vesicles. The degree of inhibition determines the quantity of PTH secretion. Once the PTH molecule is secreted, it diffuses into the capillaries and is advected away. The half-life of PTH is approximately 4 minutes [35].

Upon binding of calcium ions to the sensor's large extracellular domain [4], an

intracellular signal is generated that ultimately results in the inhibition of PTH secretion. Intracellular calcium concentrations are noted to be oscillatory in chief cells when the cells are exhibiting PTH inhibition. The total variation was in the 50 nmol/L range, with a mean amplitude 175 nmol/L. There were no oscillations noted at non-inhibitory calcium concentrations. PTH molecules are stored in intracellular vesicles (along with chromogranin A) and are exocytotically released (Figure **??**) into the extracellular space when the inhibitory signal is low.

Shoback et al. [42] show that raising extracellular [Ca2+] from 0.5 to 3.0 mM increased 3H-1,4,5-IP3 within 5 s, which was confirmed by mass measurements. 3H-1,3,4-IP3 rose and gradually increased for 60 seconds after the addition of Ca2+. This suggests that while a Ca-IP3 pathway is operant in these cells, the relationship of the Ca-IP3 system here is **the opposite of most systems** in that cell inhibition occurs during IP3-Ca stimulation. The processes of PTH exocytosis from the stored vesicles involve cell biological and biophysical factors. As described by Setoguti et al. [40] the chief cell membranes are noted to be convoluted during periods of low calcium concentration. This implies a responsive change in cell membrane shape, which is believed to be controlled by protein elements (actin) of the cell cytoskeleton [32]. It is presumed that Ca binding to the calcium sensing receptor initiates the hydrolysis of PIP2 to inosital 1,4,5 and diacylglycerol resulting in loss of PIP2 which is active in cytoskeleton-cell membrane adhesion. Thus the IP3-Ca pathway may be closely coupled with the exocytotic process.

PTH gene expression and extracellular calcium

Along with calcium, there are other molecules that influence PTH secretion including magnesium, phosphate, vitamin D and catecholamines. These are all subdominant to the effect of extracellular calcium. *In vitro* 1,25-dihydroxyvitamin D3 (1,25(OH)2D3) has been shown to decrease PTH gene transcription [24, 43]. Calcitonin is a counter regulatory hormone produced by the medullary cells of the thyroid gland. Its action provides a partial balance to the hormonal effects of PTH, though the identified target tissues are not all the same. A low cal-

cium is the major signal for PTH secretion, and a high calcium for calcitonin secretion. While calcium had no effect on calcitonin messenger RNA (mRNA) levels in vivo in the rat, a low calcium markedly stimulated PTH mRNA levels. Serum calcium was decreased by intraperitoneal phosphorus and increased by calcium gluconate. Low serum calcium markedly increased PTH mRNA levels whereas a high serum calcium had no effect. There was no change in mRNAs for calcitonin or actin in the same thyroparathyroid extracts. After phosphorus was given (intra-peritoneum), serum calcium decreased from 10.4 to 8.5 mg/dl and PTH mRNA increased up to three-fold. Gel blots showed that a low calcium increased PTH mRNA levels with no change in its size (833 base pairs). Calcitonin ip decreased both serum calcium and phosphorus with an up to five-fold increase in PTH mRNA at 1 h, thus demonstrating that the effect of phosphorus on PTH mRNA was due to the low serum calcium and not the high serum phosphorus. When phosphorus and 1,25(OH)2D3 were injected together, despite the low serum calcium, there was a decrease in PTH mRNA levels. These results show a linear relationship between calcium and PTH gene expression, but not calcitonin or actin, with a dominant role for 1,25(OH)2D3.

Diffusivity of calcium

There are scarcely few more important physical processes in biology than diffusion. It is well known from Fick's law that diffusive flux is proportional to the product of the diffusion coefficient D (diffusivity) and the local concentration gradient:

$J_A = D\frac{\partial C_A}{\partial r}$

It is often assumed that the diffusion coefficient is constant and that the effort must be placed on the concentration gradient as the driving force for transport or by reducing the path length. The study of how a particles diffusivity is affected by the solvent is traced back at least 100 years to the work of Einstein and others The hydrodynamical approach to the prediction of diffusivity are based on the Nernst-Einstein equation which relates the movement of a particle through

a liquid medium to a "resisting" force which retards the motion. When this resisting force is approximated using the Stokes drag, the model that results is commonly called the Einstein-Stokes eqation:

$$D_{AB} = \frac{KT}{6\pi\mu_B R_A}$$

Where D_{AB} is the diffusivity of solute A through Liquid B,κ is the Boltzman constant, T is temperature, μ_B is the viscosity of liquid B and R_A is the radius of solute A. This equation is valid when the solute is large paricle compared to the solvent or medium.It does not accurately describe the situation when the diffusing species is of the same size or smaller than the medium. Another approach to modeling diffusion in liquids was developed in the 1960's and was based on thr Eyring Rate theory: which explains both viscosity and diffusion on the basis of a lattice model for the liquid which contains holes. A certain activation energy is needed for diffusion and the solute can ve ienvisioned as jumping from hole to hole. Gainer and Metzner made modifications to this approach and derived the following expression for the diffusivity:

$$D_{AB} = (\frac{\kappa T}{\xi\mu_B})(\frac{N}{V_B})^{\frac{1}{3}} \exp(\frac{E_{AB}-E_{AS}}{RT})$$

where E_{AS} ,E_{AB},are the activation energies for diffusion of the free solvent and mixed solutions respectively and ξ represents the number of nearest neighbor molecules to the diffusing species. V_B is the molar volume of the solvent. Further modifications were made and it was found that the diffusivity in a polymer solution could be expressed by comparing the diffusivities of the polymer solution with that of the pure solvent. The key was that the diffusivity would be determined mostly by ΔE which is the difference in activation energies for the polymeric solution and the pure solvent. One of the first attempts to quantify this was made by Osmers in 1972. It was noted that the addition of polymer molecules to solvents should alter the intermolecular spacing in the liquid and thus affecting the activation energy difference. They further suggested that evaluating the change in the specific volume after the polymer mixing would indicate the change in the underling liqid structure. With these considerations in mind, a modification of the D_{AB} formula was obtained as is summarized below.

$$E_{AB} - E_{AS} = \Delta E$$

$$\Delta E = k\Delta V_{mix}$$

$$\frac{D_{AS}}{D_{AB}} = \exp(\alpha \Delta V_{mix}), where \qquad \alpha = \frac{k}{RT}$$

$$D_{AB} = D_{AS} \exp(-\alpha \Delta V_{mix})$$

The Diffusivity D_{AB} is therefore equal to the producuct of the free solvent diffusivity and an exponential term dependent on the difference between the activation energies of the mixed and pure solvent diffusivities. Thus, the diffusivity D_{AB} can be related to the concentration of a protein present in a biological fluid. The form of the diffusivity we use in our modeling is motivated from these considerations.

Exocytosis

The parathyroid cells release stored PTH by means of exocytosis [51]. The PTH is stored in intracellular vesicles, and as a result of a sequence of signals fuse with the cell membrane and export their contents into the interstitial spaces. The cellular processes involved in exocytosis are the subject of extensive research in cell physiology. Membrane fusion occurs as part of processes as different as synaptic neurotransmitter transmission and infection with influenza virus. Recent evidence paints a picture in which the organization of proteins into a macro molecular scaffold brings the two fusing membranes together to form a common bilayer. A small dynamic fusion pore forms in the common bilayer and usually expands to allow complete membrane merging (see Figure 9.3). The mechanisms of fusion appear to be remarkably similar in exocytosis and virus-induced fusion. During exocytotic fusion, there is an additional twist to the mechanism, as sometimes the fusion pores close after release of small non-quantal amounts of secretory products.

PTH secretion *In VITRO*

In a 1993 JCI article, Sun et al. [44] demonstrated that the PTH secreting cells in an individual parathyroid gland have a heterogeneous response to calcium. The

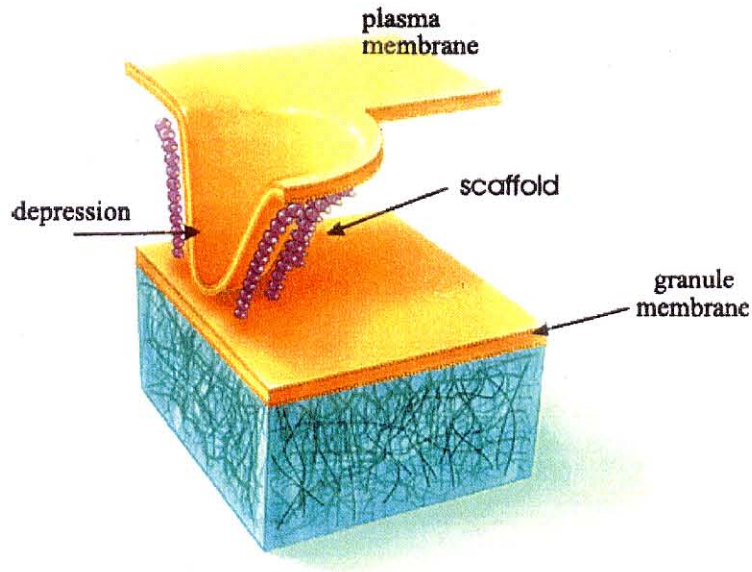

Figure 9.3: A schematic of a fusion pore being formed.

number of cells responding to a 1.5 mmolar Ca conc. was 30% and that increased to 50% at 0.1 mmolar and fell to 20% at 2 mmolar. The conclusion drawn is that there is a distribution of set points or thresholds for the calcium/PTH response in the gland population. There are no reports of PTH molecules having autocrine function; however, co-released chromogranin-A may degenerate and break down into pancreastatin, which is known to inhibit PTH secretion. This process has been shown to take place on the order of 30-60 minutes according to some published studies [12].

Sun et al. observed that cell-cell spacing effected PTH secretion [45]. Increasing cell population density corresponded with increased PTH production. The PTH conditioned media was consequently tested in primary cultures of bovine parathyroid gland and shown not to have any effect on increasing PTH secretion. A related study from the same group [46] demonstrated that single isolated PTH secreting cells were inhibited at lower concentrations of calcium then were clusters of cells; however, the amount of PTH secreted per cell was higher in the group than in the isolated individual [13]. There are numerous accounts of this type of group versus single isolated cell behavior. The pancreatic islet cells and cells from the anterior pituitary gland are prominent examples. The fact that

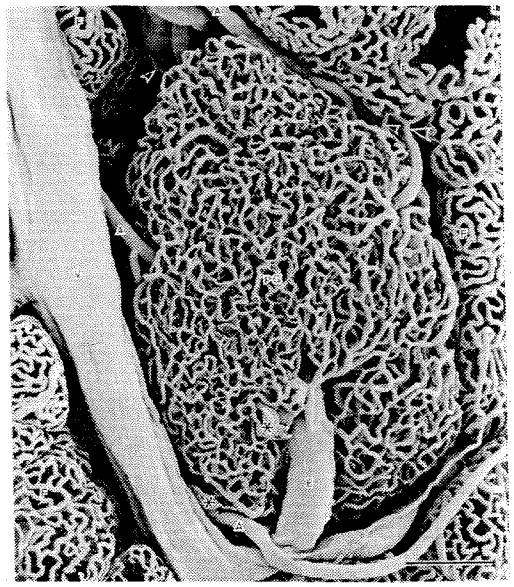

Figure 9.4: The parathyroid gland has a very rich vasculature as seen from this prepared vascular cast.

increased crowding was correlated to increased in vitro secretion of PTH lends consistency to the result reported by Yu et al. [54]. In that study, a fixed calcium concentration is applied to adenomatous tissue *in vitro*. The adenomatous cells resist the calcium inhibitory effect, much the same way they do in clinical syndromes of primary hyperparathyroidism. The recovery of calcium sensitivity upon dispersion of these cells into smaller fragments was unexpected and remained unexplained.

Finally, Rithchie et al. [33] report that chief cells exhibit cyclic secretion. Chief cells that are observed to be initially PTH secreting will convert to non-secreting status 1/4 of the time, while non-secretors convert to secretors 1/2 the time.

Anatomy and histology

The parathyroid glands develop from the 3rd and 4th pharyngeal pouches in the 5th week of embryonic life. In most healthy humans there are four glands of approx. (3mm x 7mm x .5mm) size (Figure 1.1). They are located in the neck and attached to the thyroid gland [51]. The glandular architecture is arranged in chords or nests of cells surrounded by capillaries (Figure 9.4) [47]. The parathyroid gland geometry is segmented into nests or chords of cells surrounded by a

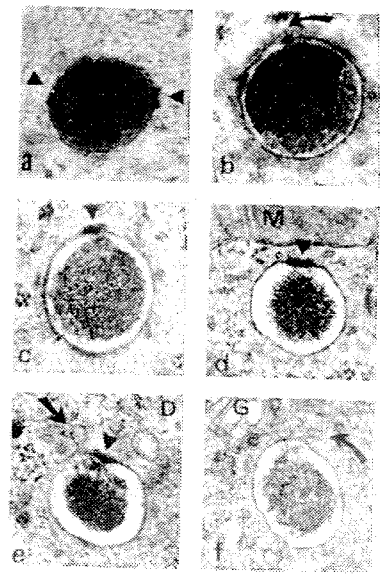

Figure 9.5: Storage granules in different stages of their life cycle.

capillary network [47]. The apical portions of a typical chief cells face inwardly toward other chief cells while the basal portion is often positioned near a capillary. The cells have been reported to have an apical-lateral secretory polarity [49]. (Figure ??). The PTH secreting cells (chief cells) can be seen to have villi like structures on plasma membranes in the apical lateral regions. The "villi" formation is decreased in the presence of higher extracellular calcium concentration. Intra-cellular vesicles containing PTH are usually categorized into two types: Type I an early vesicle and Type II mature [40, 21, 48]. The vesicle number is observed to change corresponding extracellular calcium levels. (Figure 9.5). In one study by Setoguti et al. [41], type I vesicles reached a minimum in 30 minutes following the change of the ambient calcium from 9 mg/dl to 13.2 mg/dl.

The histopathological distinction between normal, hyperplastic and adenomatous tissue is not always straightforward. Adenomatous cells are larger and possess an abundant cytoplasm compared with normal cells. The adenomas are organized in dense sheets that crowd adjacent normal cells [51].

Pathology and pathophysiology

An important physiological difference between normal cells and hyperplastic or adenomatous cells is a shift in the ability to suppress PTH secretion. Much higher levels of [Ca] are needed to suppress the secretion of PTH in hyperplasia and adenoma [15, 37]. Additionally the pathological cells respond to changes in extracellular calcium with smaller than normal increments. There is some evidence pointing to changes in intracellular calcium signaling and the amount of calcium sensor protein on the cell surface [22].

Excess PTH secretion or hyperparathyroidism is most commonly caused by adenomas (80%) and hyperplasia (20%). Parathyroid adenomas are caused by somatic mutations in parathyroid cells. Subsequent clonal expansion results in the tumor. Multiple chromosomal regions have been shown to be missing in adenomatous cells. Hyperplasia is thought to be a result of polyclonal expansion [51].

Bibliography

[1] R.G.W. Anderson. "The Caveolae Membrane System." *Annu. Rev. Biochem.* **67**: 199-225 (1998)

[2] G.K. Batchelor. "An Introduction to Fluid Dynamics." *Cambridge Univ. Press.* (1999)

[3] G.A. Brent. "Relationship between the concentration and rate of change of calcium and serum intact parathyroid homone levels in normal humans." *J. Cinical Endocrinol. Metab.* **67**: 944, (1988)

[4] A.J. Brown, C.S. Ritter, J.L. Finch, and E.A. Slatopolsky. "Decreased calcium-sensing receptor expression in hyperplastic parathyroid glands of uremic rats: Role of dietary phosphate." *Kidney International* **55(4)**: 1284-92. (1999)

[5] N. Chattopadhyay. *Int. J. Biochem. Cell Biol.*. **32 (8)**: 789-804 (Aug. 2000)

[6] C.J. Chen, C.S. Anast, and E.M. Brown. "High Osmolality: A potent parathyroid hormone secretogogue in dispersed parathyroid cells." *Endocrinology* **121**: 958-964 (1986)

[7] D.S. Cohen. "Inaccessible states in time-dependent reaction-diffusion." *Studies in Applied Math.* **97**: 301-319 (1996)

[8] D.S. Cohen, and D.A. Edwards. "The effect of a changing diffusion coefficient in super-case II polymer-penetrant systems." *IMA J. of Applied Math.* **55**: 49-66 (1995)

[9] F.S. Cohen, M.H. Akabas, and A. Finkelstein. "Osmotic swelling of phospholipid vesicles causes them to fuse with a planar phospholipid bilayer membrane." *Science* **217**: 458-460 (1982)

[10] P.R. Conlin, V.T. Fajtova, R.M. Mortensen, M.S. LeBoff, and E.M. Brown, "Hysteresis in the relationship between serum ionized calcium and intact parathyroid hormone during recovery from induced hyper-and hypocalcemia

in normal humans." J. of Clinical Endocrinology and Metabolism **69(3)**: 593-599 (1989)

[11] J. Crank. "The Mathematics of Diffusion." *Oxford Science Publications* (1995)

[12] B.M. Drees, and J.W. Hamilton. "Pancreastatin and bovine parathyroid cell secretion." *Bone and Mineral* **17**: 335-346 (1992)

[13] L.A. Fitzpatrick, and D.A. Leong. "Individual parathyroid cells are more sensitive to calcium than a parathyroid cell population." *Endocrinology* **126 (3)**: 1720-1727 (1990)

[14] J.L. Gainer. "Altering diffusivities in dilute polymeric and biological solutions." *Ind. Eng. Chem. Res.* **33**: 2341-2344 (1994)

[15] W.G. Goodman, J.D. Veldhuis, T.R. Belin, A.J. VanHerle, H. Juppner, and I.B. Salusky. *Journal of Clin Endocrinol Metab* **83**: 2765-2772 (1998)

[16] H.M. Harms, U. Kaptaina, W.R. Kulpmann, G. Brabant, and R.D. Hesch. *J. Clin. Endocrinol. Metab.* **69(4)**: 843-851 (Oct. 1989)

[17] H.M. Harms, O. Neubauer, C. Kayser, P.R. Wustermann, R. Horn, U. Brosa, E.Schlinke, W.R. Kulpmann, A. von zur Muhlen, and R.D. Hesch. *J. Clin. Endocrinol. Metab.* **78(1)**: 48-52 (Jan. 1994)

[18] C. Ho, D.A.Conner, M.R. Pollak, D.J. Ladd, O. Kifor, H.B. Warren, E. M. Brown, J. G. Seidman, and C. E. Seidman. *Nat. Genet.* **11(4)**: 389-94 (1995)

[19] K.L. Hyrc, J.M. Bownik, and M.P. Goldberg. "Neuronal free calcium measurement using BTC/AM, a low affinity calcium indicator." *Cell Calcium* **24 (3)**: 165-175 (1998)

[20] C. Juhlin, J. Rastad, L. Klareskog, L. Grimelius, and G. Akerstrom. "Parathyroid histology and cytology with monoclonal antibodies recognizing a calcium sensor of parathyroid cells." *Amer. J. of Pathology* **135 (2)**: 321-328 (1989)

[21] C. Kaneko, K. Mizunashi, M. Tanaka, M. Uzuki, M. Kikuchi, T. Sawai, and M.M. Goto. "Relationship between Ca-dependent change of serum PTH and

Extracellular $Ca^2\pm$ sensing receptor expression in parathyroid adenoma." *Calcif. Tissue Int.* **64**: 271-272 (1999)

[22] O. Kifor, R. Diaz, R. Butters, I. Kifor, and E.M. Brown. *J. Biol. Chem.* **273(34)**: 21708-13 (1998)

[23] K.E. Laidig, J.L. Gainer, and Daggett, V. "Altering diffusivity in biological solutions through modification of solution structure and dynamics." *J. Am. Chem. Soc.* **120**: 9394-9395 (1998)

[24] T. Naveh-Many, M.M. Friedlaender, H. Mayer, and J. Silver. *Endocrinology* **125(1)**: 275-80 (Jul. 1989)

[25] E.F. Nemeth, M.E. Steffey, L.G. Hammerland, B.C. Hung, B.C. Van Wagenen, E.G. DelMar, and M.F. Balandrin. *Proc. Natl. Acad. Sci. USA* **95(7)**: 4040-5. (Mar. 31, 1998)

[26] C. Nicholson, J.M. Phillips, and A.R. Gardner-Medwin. "Diffusion from an iontophoretic point source in the brain: role of tortuosity and volume fraction." *Brain Research* **169**: 580-584 (1979)

[27] C. Nicholson, and J.M. Phillips. "Ion diffusion modified by tortuosity and volume fraction in the extracellular microenvironment of the rat cerebellum." *J. Physiol.* **321**: 225-257 (1981)

[28] C. Nicholson, and M.E. Rice. "Calcium diffusion in the brain cell microenvironment." *J. Physiol. Pharmacol.* **65**: 1086-1091 (1987)

[29] C. Nicholson, and E. Sykova. "Extracellular space structure revealed by diffusion analysis." *Trends Neurosci.* **21**: 207-215 (1998)

[30] "Numerical Recipes in Fortran." (W. Press ed.) 2nd edition *Cambridge Press* (1992)

[31] A. Pluen, Y. Boucher, S. Ramanulan, T.D. McKee, T.E. Gohongi, E. Brown, Y. Izumi, R.B. Campbel, D.A. Berk, and R.K. Jain. *Proc. Natl. Acad. Sci. USA* **98**: 4628-4633 (2001)

[32] D. Raucher, and M.P. Sheetz. "Cell spreading and lamellipodial extension rate is regulated by membrane tension." *J. Cell Biol.* **10 148(1)**: 127-36 (Jan. 2000)

[33] C.K. Ritchie, D.V. Cohn, P.B. Maercklein, and L.A. Fitzpatrick, "Individual parathyroid cells exhibit cyclic secretion of parathyroid hormone and Chromagranin-A (as measured by a novel sequential hemolytic plaque assay)." *Endocrinology* **131 (6)**: 2638-2642. (1992)

[34] D.A. Rusakov, and D.M. Kullmann. "Geometric and viscous components of the tortuosity of the extracellular space in the brain." *Neurobiology* **95 (15)**: 8975-8980. (1998)

[35] H. Saha, A. Harmoinen, K. Pietila, P. Morsky, and A. Pasternack. *Clin. Nephrol.* **46 (5)**: 326-31 (Nov. 1996)

[36] R. Samtaney *ASCI program at Caltech.* (2000)

[37] C.P. Schmitt, D. Huber, O. Mehls, J. Maiwald, G. Stein, J.D. Veldhuis, E. Ritz, and F. Schaefer. *J. Am. Soc. Nephrol.* **9(10)**: 1832-1844 (Oct. 1998)

[38] P.S. Schmitt, F. Schaeffer, A. Bruch, J.D. Veldhuis, et al. "Control of pulsatile and tonic parathyroid hormone secretion by ionized calcium." *J. Clin. Metab.* **81**: 4236-4243 (1996)

[39] P. Schwarz, J.C. Madsen, A.Q. Rasmussen, L.B. Transbol, and E.M. Brown. "Evidence for a role of intracellular stored parathyroid hormone in producing hysteresis of the PTH-calcium relationship in normal humans." *Clinical Endocrinology* **48**: 725-732 (1998)

[40] T. Setoguti, Y. Inoue, and M. Shin. "Effects of short-term treatment with calcium on the parathyroid gland of the rat, under particular consideration of the alteration of storage granules." *Cell Tissue* **240**: 9-17. (1985)

[41] T. Setoguti, Y. Inoue, and P. Wild. "The biological significance of storage granules in rat parathyroid cells." *Microscopy Research and Technique* **32**: 148-163 (1995)

[42] D.M. Shoback, T.H. Chen, B. Lattyak, K. King, and R. Johnson. "Effects of high extracellular calcium and strontium on inositol polyphosphates in bovine parathyroid cells." *J. Bone Miner Res.* **8(7)**: 891-8 (July 1993)

[43] E. Slatopolsky, A. Brown, and A. Dusso. *Am. J. Kidney Dis.* **37(1 Suppl 2)**: S54- (Jan. 2001)

[44] F. Sun, P. Maercklein, and L.A. Fitzpatrick. *J. Bone Miner. Res.* **7**: 971-6 (1994)

[45] F. Sun, P. Maercklein, and L.A. Fitzpatrick. "Paracrine interactions among parathyroid cells: Effect of cell density on cell secretion." *Div. Of Endocrinology, Dept. of Medicine, Mayo Clinic and Mayo Foundation* (1993)

[46] F. Sun, C.K. Ritchie, C. Hassager, P. Maercklein, and L.A. Fitzpatrick. "Heterogeneous response to calcium by individual parathyroid cells." *J. Clin. Invest.* **91**: 595-601. (1993)

[47] T. Tanaka, M. Tsubouchi, Y. Tsubouchi, A. Ohtsuka, and T. Murakami. "Rat parathyroid gland, with special reference to its blood vascular bed, pericapillary space and intercellular space." *Acta Med Okayama* **50 (5)**: 243-253 (1996)

[48] A. Wernerson, O. Svensson, and F.P. Reinholt. "Quantitative and three-dimensional aspects of the rat parathyroid gland in normo-, hypo-, and hypercalcemia." *Microscopy Research and Technique* **32**: 129-147. (1995)

[49] P. Wild, and E.M. Schraner. "Parathyroid cell polarity as revealed by cytochemical localization of ATPases, alkaline phosphatase and $5'-$nucleotidase." *Histochemistry* **94**: 409-414 (1990)

[50] C.R. Wilke, and P. Chang. "Correlation of diffusion coefficients in dilute solutions." *A.I.Ch.E. Journal* **1 (2)**: 264-270 (1995)

[51] Williams Textbook in Endocrinology (Wilson J ed.) 1998 WB Saunders Co.

[52] K.L. Yam, D.K. Anderson, and R.E. Buxbaum. "Diffusion of small solutes in polymer-containing solutions." *Science* **241 (4863)**: 330-332. (1988)

[53] M. Yamamoto, T. Igarashi, M. Muramatsu, M. Fukagawa, T. Motokura, and E. Ogata. *J. Clin. Invest.* **83(3)**: 1053-6 (Mar. 1989)

[54] M. Yu, H.M. Van Herle, J.D. Lin, A.E. Giuliano, and A.J. Van Herle. "Differences in PTH (1-84) realease in response to ambient calcium concentrations of parathyroid adenoma fragments and dispersed parathyroid adenoma cells in culture." *J. Endocrinol. Invest.* **19**: 342-347 (1996)